(2)

PL-TR-92-2006

CLUSTER ANALYSIS OF CLOSELY SPACED MINING BLASTS AS A METHOD OF EVENT LOCATION

Florence Riviere-Barbier
Lori Teresa Grant

Science Applications International Corporation
Center for Seismic Studies
1300 N. 17th Street, Suite 1450
Arlington, VA 22209

30 January 1992

Final Technical Report
1 October 1990 - 1 October 1991

Approved for public release; distribution unlimited

PHILLIPS LABORATORY
AIR FORCE SYSTEMS COMMAND
HANSCOM AIR FORCE BASE, MASSACHUSETTS 01731-5000

SPONSORED BY
Defense Advanced Research Projects Agency
Nuclear Monitoring Research Office
ARPA ORDER NO. 5307

MONITORED BY
Phillips Laboratory
Contract F19628-88-C-0159

This technical report has been reviewed and is approved for publication.

JAMES F. LEWKOWICZ
Contract Manager
Solid Earth Geophysics Branch
Earth Sciences Division

JAMES F. LEWKOWICZ
Branch Chief
Solid Earth Geophysics Branch
Earth Sciences Division

DONALD H. ECKHARDT, Director
Earth Sciences Division

REPORT DOCUMENTATION PAGE

Form Approved
OMB No. 0704-0188

1. AGENCY USE ONLY *(Leave blank)*

2. REPORT DATE
30 January 1992

3. REPORT TYPE AND DATES COVERED
Final (1 Oct 1990-1 Oct 1991)

4. TITLE AND SUBTITLE
Cluster Analysis of Closely Spaced Mining Blasts as a Method of Event Location

5. FUNDING NUMBERS
PE 62714E
PR 8A10 TA DA WU AT
Contract F19628-88-C-0159

6. AUTHOR(S)
Florence Riviere-Barbier
Lori Teresa Grant

7. PERFORMING ORGANIZATION NAME(S) AND ADDRESS(ES)
Science Applications International Corporation
Center for Seismic Studies
1300 N. 17th Street, Suite 1450
Arlington, VA 22209

8. PERFORMING ORGANIZATION REPORT NUMBER

9. SPONSORING/MONITORING AGENCY NAME(S) AND ADDRESS(ES)
Phillips Laboratory
Hanscom AFB, MA 01731-5000

Contract Manager: James Lewkowicz/GPEH

10. SPONSORING/MONITORING AGENCY REPORT NUMBER
PL-TR-92-2006

11. SUPPLEMENTARY NOTES

12a. DISTRIBUTION/AVAILABILITY STATEMENT
Approved for public release;
Distribution unlimited

12b. DISTRIBUTION CODE

13. ABSTRACT *(Maximum 200 words)*
This is the Final Report of contract F19628-88-C-0159, Analysis of High Frequency Seismic Data. The aim of the research conducted under this contract was to characterize the high frequency content of noise and signals, and to develop methods of discriminating between mine blasts and other seismic sources using high frequency seismic data. Two previous reports (Israelsson et al., 1990; and Israelsson and Carter, 1991) describe much of the research conducted under this contract and covered the high frequency characteristics of local, regional, and teleseismic waveforms as recorded at the short period Scandinavian arrays and the NRDC high frequency stations in the Soviet Union.

The final six months of the contract were devoted to a study of mining event characterization for location and discrimination purposes. Cluster analysis was used to group events with similar characteristics from the mining district of Karelian, northwest of St. Petersburg. The groupings compared well with a careful visual classification of the same data and were hypothesized to be associated with
(continued on reverse)

14. SUBJECT TERMS

FINESA	Cluster analysis	IMS
ARCESS	f-k analysis	
NORESS	Cross-correlation	

15. NUMBER OF PAGES
54

16. PRICE CODE

17. SECURITY CLASSIFICATION OF REPORT	18. SECURITY CLASSIFICATION OF THIS PAGE	19. SECURITY CLASSIFICATION OF ABSTRACT	20. LIMITATION OF ABSTRACT
Unclassified	Unclassified	Unclassified	SAR

13. Abstract (continued)

specific mines. The results of this study are very promising and warrant expanding to other mining districts. Future studies based on this work, however, should verify the event sources using non-seismic data before an absolute event identification is assigned.

TABLE OF CONTENTS

LIST OF FIGURES

LIST OF TABLES

FOREWORD

This is the Final Report of contract F19628-88-C-0159, Analysis of High Frequency Seismic Data. The aim of the research conducted under this contract was to characterize the high frequency content of noise and signals, and to develop methods of discriminating between mine blasts and other seismic sources using high frequency seismic data. Two previous reports (Israelsson *et al.*, 1990; and Israelsson and Carter, 1991) describe much of the research conducted under this contract and covered the high frequency characteristics of local, regional, and teleseismic waveforms as recorded at the short period Scandinavian arrays and the NRDC high frequency stations in the Soviet Union.

Much of the work presented in the previous reports contributed to the mine characterization study described herein. The material covered in Israelsson *et al.* (1990) showed evidence that shooting practices at the Kola Peninsula mines is different than at the Scandinavian mines. Studies were also made of event characterization using spectrograms (in an attempt to characterize events with spectral scalloping) and waveform correlation of closely spaced events. The spectral scalloping study showed that while spectral scalloping was evident for some mine blasts, it was not a consistent feature. Waveform correlation, on the other hand, showed promise as a method for grouping events from a specific mine and was adopted in a modified form for this final study. Israelsson and Carter, (1991) contains studies on the high frequency content of teleseismic P-waves; estimating the characteristics of ripple-fired explosions; and slowness estimation with interpolated NORESS data. The slowness estimation study was able to discern differences in the wave-fronts of the first arrivals from the northeast and southwest sections of the Balapan test site using interpolated NORESS data.

The final six months of the contract were devoted to a study of mining event characterization for location and discrimination purposes. Cluster analysis was used to group events with similar characteristics from the mining district of Karelian, northwest of St. Petersburg. The groupings compared well with a careful visual classification of the same data and were hypothesized to be associated with specific mines. The results of this study are very promising and warrant expanding to other mining districts. Future studies based on this work, however, should verify the event sources using non-seismic data before an absolute event identification is assigned.

INTRODUCTION

Numerous discrimination studies have been performed to distinguish between events of different source type (Blandford, 1982; Pomeroy *et al.*, 1982). The initial studies used modeling in an attempt to reproduce the effects of the source on the signal or spectrum. More recent studies used a case-based approach and tried to parameterize the signal and spectrum. Studies of frequency content in order to detect "ripple firing" (Baumgardt and Ziegler, 1988; Smith, 1989) showed that spectral modulations could be used to distinguish mine blasts from earthquakes and nuclear explosions. Dysart and Pulli (1989) characterized chemical explosions and earthquakes recorded at the NORESS array using amplitude ratios and spectral complexity. Israelsson (1990), in an application of cluster analysis to the discrimination problem, was able to distinguish closely spaced events located within an area of 20 km by 75 km by taking advantage of the repeatability of signals from similar sources. In general, these studies showed that methods used to discriminate events should be applied at regional distances so that the tectonic environment is integrated (Bennett *et al.*, 1989).

The purpose of this study is to characterize and distinguish between mines located within a few kilometers of each other. This characterization may then be implemented in an automatic detection, location, and discrimination system such as the Intelligent Monitoring System (IMS) (Bache *et al.*, 1990). A discrimination method that can associate events with a particular mine will reduce the number of events that need to be investigated in more detail.

The IMS processes data from four arrays (ARCESS, NORESS, FINESA and GERESS) providing a large data set of local and regional events from the baltic shield and the western part of the east-european platform (*Figure 1*). An automatic location is computed for each event which is later reviewed by an analyst. Even when an event location is constrained by data from three different arrays, the error ellipse can be large enough to include several mines. The average estimated error of the IMS locations is 20 km (Bratt *et al.*, 1990).

Three different areas with a high concentration of mines in the local to regional distance range from the IMS arrays were identified in the Russian territories closest to Finland. Two areas are located near St. Petersburg and the third one includes mines on the Kola Peninsula. This paper is devoted to the results obtained for the mining district located north of St. Petersburg, in Karelian.

The discrimination technique used for this study is a cluster analysis method (Everitt, 1986) based on waveform similarity. It does not require any pre-classification of events into groups.

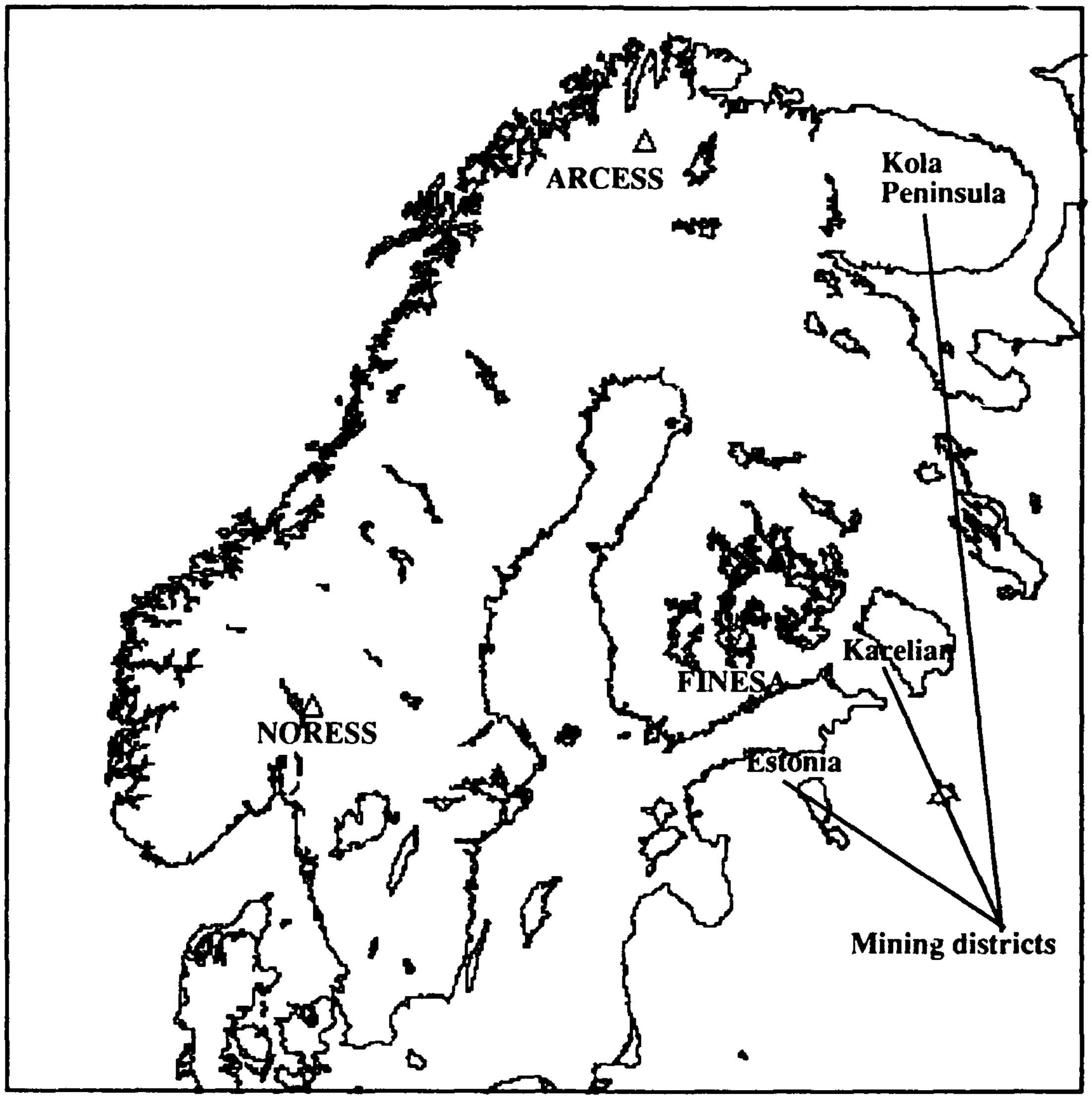

Figure 1: Location of ARCESS, FINESA and NORESS arrays collecting the data processed by the Intelligent Monitoring System. ARCESS and NORESS are located in Norway while FINESA is located in Finland. Three important mining districts have been identified: in Estonia, in Karelian, and on the Kola Peninsula.

DATA

The data set covers the period of time from November 4, 1990 to June 28, 1991. Waveforms recorded at FINESA, ARCESS and NORESS as well as phase parameters computed and saved during the automatic detection and location of events by the IMS were utilized in this study. The set of phase parameters extracted from the IMS database was similar to the set used by Baumgardt (1987).

Waveforms

Waveforms used in this study were automatically saved on optical disk by the IMS. Since November 4, 1990, all waveforms with at least one associated phase after analyst review have been archived, unless a software failure caused a loss of data.

Database Parameters

Only events with at least one *Pn* or *Pg* and one *Lg* phase were considered. For each phase, the following parameters were extracted from the IMS parameter database:

- detection time
- azimuth computed from *f-k* analysis
- velocity computed from *f-k* analysis
- center period of the phase
- short term average measured on the incoherent vertical beam filtered between 2 and 4 Hz.

The detection time was used to compute a "relative time". This relative time was defined as the time difference between the earliest phase detected at any of the stations and the detection time of the other phases (Bache *et al*,1990). The short term average (sta) values were used in a ratio: sta(*Pn*)/sta(*Lg*) computed in decibels. Additional polarization parameters such as azimuth and rectilinearity for the *P*-type phase, horizontal-to-vertical ratio for *P*-type and *S*-type phases, and planarity for the *S*-type phases were added to the set of parameters described above.

Event locations

In addition to the IMS bulletin, a source of accurate locations for small events in this area is the bulletin published by the University of Helsinki (Uski *et al.*, 1990). Monthly bulletins are released several months after the events occur. A weekly bulletin is released earlier.

Fewer events were reported in the Helsinki bulletin than in the IMS bulletin as the Helsinki bulletin did not report most of the events with an IMS magnitude below 1.2 (*Figure 2*). Of the 55 events not reported in the Helsinki bulletin, only seven had an IMS magnitude greater than 1.2. Most of the events with a magnitude between 1.2 and 1.8 in the Helsinki bulletin had a "manual location" which means that the Finnish analyst assigned them to a particular mine by visual inspection. An automatic location was reported for the events with an IMS magnitude above 1.8 and included information from other stations in the Nordic countries. The IMS location included information from only the FINESA array for small events or from all three arrays (ARCESS, NORESS, FINESA) for larger events (usually with a local magnitude above 1.5).

MINE LOCATIONS

Table 1: Mine Locations from the Helsinki bulletin (Hels.) and SPOT photos (Fox, 1990).

Hels.	lat.	lon.	azim.	dist.	SPOT	lat.	lon.	azim.	dist.
HC1	60.7°	28.7°	119.2°	1.48°	SC1	60.749°	28.836°	116.3°	1.51°
HC2	60.7	29.0	116.47	1.60	SC2	60.700	29.181	114.99	1.68
HC3	60.6	29.2	117.78	1.74	SC3	60.581	29.065	119.48	1.69
HC4	60.8	29.3	111.06	1.69	SC4	60.846	28.99	111.76	1.53
HC5	60.9	29.3	107.88	1.65	SC5	61.008	29.038	105.71	1.50
HC6	60.9	29.4	107.29	1.70	SC6	60.953	29.176	106.84	1.58
HC7	60.8	29.5	109.78	1.78	SC7	60.902	29.348	107.53	1.67
HC10	61.1	29.9	98.93	1.88					
HC11	61.1	30.2	98.04	2.00	SC11	61.142	29.870	97.75	1.85
HC12	61.5	30.4	86.56	2.07					
HC13	61.9	30.6	76.05	2.20					
HC14	61.4	31.6	88.54	2.65	SC14	61.605	31.424	84.06	2.57
HB15	60.0	29.9	125.99	2.37	SB15	60.019	29.742	126.87	2.30
N114	61.03	28.18	111.34	1.10					
N117	61.9	29.0	70.55	1.47					

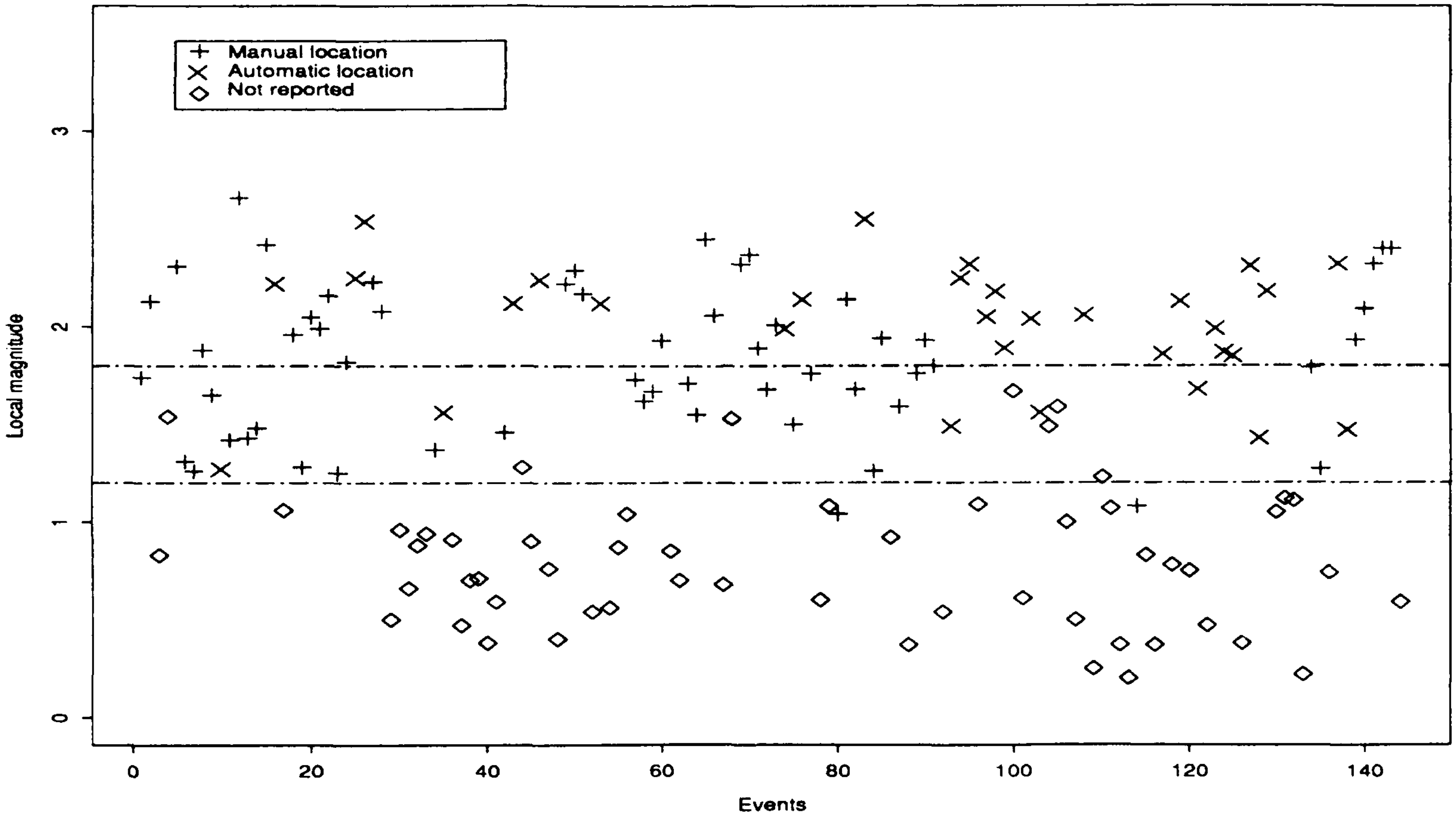

Figure 2: Magnitudes reported in the Helsinki bulletin for 89 of the studied events. Many of the events for which the IMS magnitude was above 1.8 were located using an automatic process. Only a few events with an IMS magnitude below 1.2 were reported in the Helsinki bulletin. For the remaining events, a "manual location" was reported that corresponded to a mine location. The Finnish analysts routinely recognize and "manually locate" recurring mining blasts close to their stations.

Table 1 is a list of the mine locations available for the area. The Helsinki bulletin made reference to 15 mines in this area during this time period. The left half of the table corresponds to the locations found in the Helsinki bulletin. The right half of the table gives information compiled by Fox (1990) using satellite photos. Helsinki mine locations have been determined seismically by averaging repeated events. The accuracy of these locations is only given to one-tenth of a degree. Some locations clearly include several small mines about 2.5 km apart. According to the scientists at the University of Helsinki, locations of events outside of the Finnish network are not considered accurate to better than 5 km. An attempt was made to provide an equivalent SPOT location for each Helsinki mine. SPOT locations can be an average location that includes several small mines. Most SPOT locations have a corresponding Helsinki location; however, a few Helsinki mine locations do not have a corresponding SPOT location *(Figure 3)*

ANALYSIS METHODS

Cluster analysis

In order to characterize and classify the mining events from a small area, a method was required that could distinguish the subtle differences between closely spaced events. The ability of the method to work in an automated system was also considered. Cluster analysis was chosen for the task as it provided a method of grouping events based on an comparison of event pairs. The result of each comparison was reduced to a single number, the collection of which constituted the elements of a matrix used by the cluster analysis.

Cluster analysis can be based on the comparison of either "distance" or "similarity" between data (Everitt, 1986). Distance values are greater than or equal to zero. Similarity values range from zero to one. In a distance scheme, data that are similar are assigned a small distance value and data that are dissimilar are assigned large distance values. The opposite is true for similarity measurements. A similarity measurement was applied to the waveforms while a distance measurement was more appropriate for parameter data. The results of either measurement are represented by a cluster tree or dendogram.

Among the several methods used to build cluster trees, the most popular are the *complete linkage* method and the *single linkage* method. The results of these clusters can be quite different. In the *single linkage* method, distance between groups is defined as the distance between the closest members while in the *complete linkage* method, this distance is defined as the distance between the furthest members. The results presented in this paper were better represented by the *complete linkage* method because it handles problematic data better (i.e. multiple events). Several similarity measurements were tried and are

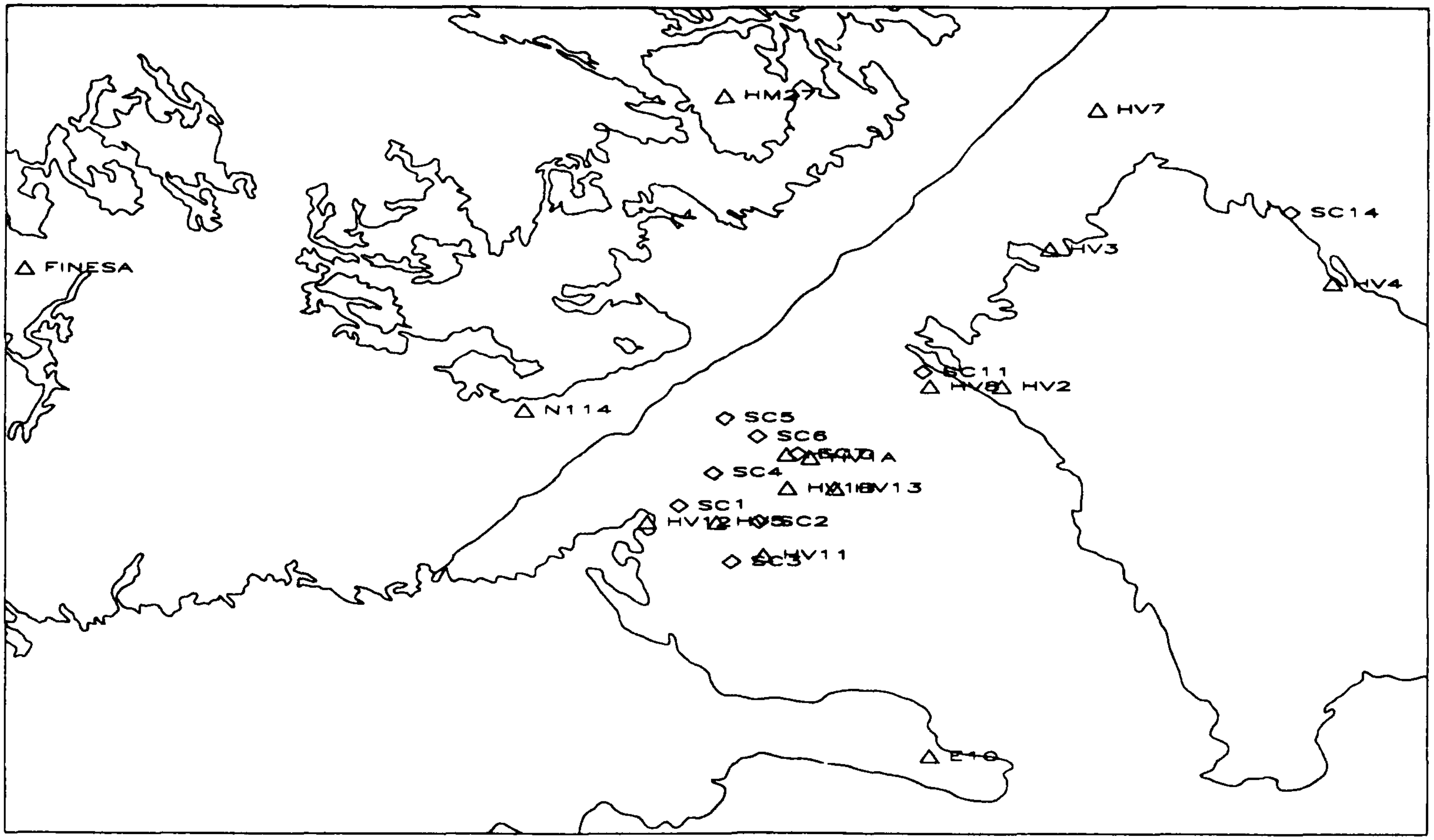

Figure 3: Comparison between mine locations determined using Helsinki seismic data (HC1 to HC14) and the locations determined on SPOT photos by Fox (1991). Helsinki locations have been determined seismically and an attempt has been made to provide an equivalent SPOT location for each of them. A SPOT location can include several small mines within a few kilometers of each other.

described below.

Cross-correlation

By assuming that events from the same mine should look very similar, the computation of cross-correlation values provides an easy way to build a numerical link between similar events. A high cross-correlation value between two events would imply a high probability that the events were from the same mine. A cross-correlation function was computed between each pair of events using signals recorded on the sz channel (FIA1 sensor) at FINESA. The input to the cluster analysis was a symmetric n × n matrix where n was the number of events. The elements of the matrix were the maximum values of the cross-correlation function.

Waveforms recorded at FINESA from the Karelian mines were studied because the signal-to-noise ratio was higher than for the data recorded at ARCESS or NORESS. Different data processing techniques were tested before computing the cross-correlation function. Raw data, filtered data, and the envelope of either unfiltered or filtered data were tried using sz, sn and se components either separately or in combination. Different signal lengths were tested including the entire signal, only *P*, and only *Lg*. The best results were obtained for the cross-correlation between the envelope (from the Hilbert transform) of the entire signal on the sz component. When the signal-to-noise ratio was low, best results were obtained with signals filtered between 1 and 15 Hz.

Other similarity measurements

The method described by Israelsson (1990) was based on a covariance matrix which was built for each component pair and each event. The six covariance matrices were stacked for each event and a cross-correlation was computed for each pair of stacked traces. This method was tested but did not provide more accurate results than the cross-correlation between envelopes.

Another similarity measurement was made using the maximum value of the coherence between pairs of events. Two different methods were used to pick this maximum value. In one method, the maximum of the entire coherence function was used; and in the other method, the maximum was picked in the frequency band that showed the best signal-to-noise ratio. Neither method was successful because there was little coherent energy above the noise between event pairs and it was difficult to find a consistent frequency band from event to event that provided useful results.

Distance measurements

In an attempt to use data parameters, relations between events were better represented by a distance measurement. The set of phase parameters characterizing each event was used to compute a "distance" value between each pair of events. The data were first normalized as the parameters did not have the same units. Then, a principal component analysis was performed on the data to eliminate any redundant information. Finally, an euclidean distance (Everitt, 1986) was computed for each pair of events that were used in the cluster analysis.

Visual classification

In order to better interpret and verify the results of the cluster analysis, a visual classification was performed using recordings of the vertical channel. The visual classification was based on the following characteristics listed in order of importance:

- *Lg* - *P* time,
- *Rg* - *P* time,
- similarity in the shapes of the *P* arrivals for the first three seconds,
- similarity in the shapes of the *Lg* and/or the *Rg* phases,
- superposition of the waveforms for each phase,
- frequency content.

The visual classification using filtered and unfiltered data sometimes resulted in different groupings for events from closely spaced mines. The classification based on unfiltered data (when the signal-to-noise ratio was high enough) was preferably used.

Interactive f-k analysis

An *f-k* analysis was performed interactively on most of the events using all eighteen sz channels of the FINESA array. The aperture of the array is 2 km. An apparent velocity (from a slowness) and an azimuth were obtained for each of the studied events. In this way, a coherent beam was calculated for each event. The purpose of this analysis was to see if these *f-k* results could provide event locations that were accurate enough to associate events to specific mines. Azimuth and slowness values obtained by the IMS using automatically picked phases did not provide sufficient accuracy.

FINESA RESULTS

Seven months of FINESSA data were searched for events that occurred within the area between 60 and 62° latitude, and 28 and 32° longitude. One hundred and forty-four events met these criteria and were used in the cross-correlation and cluster analysis computations. The IMS locations of the events are plotted in *Figure 4* and listed in Table 2.. The IMS local magnitudes ranged between 0.22 and 2.66. The distance from FINESA was between

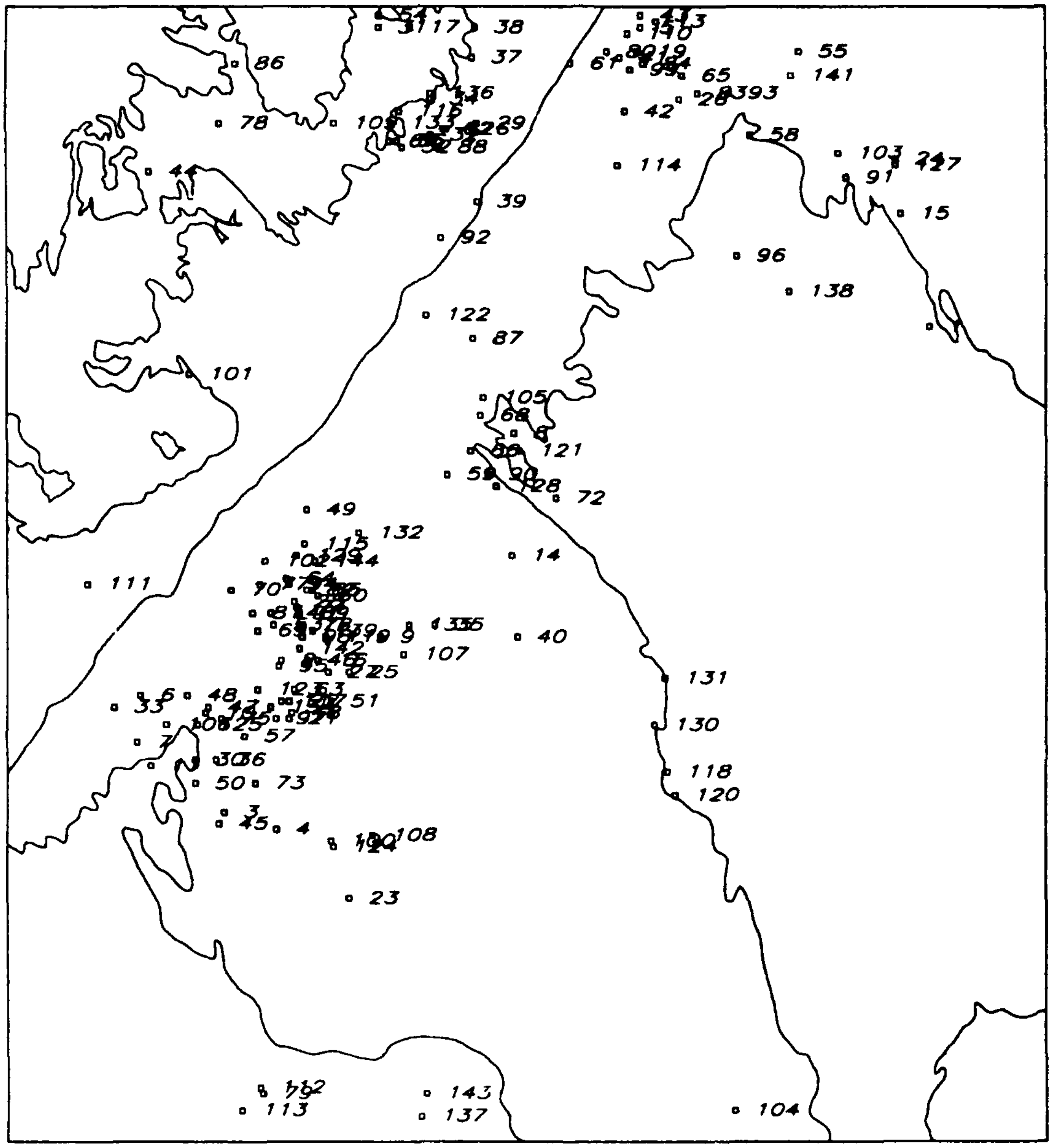

Figure 4: One hundred-forty-four events recorded at FINESA were studied and classified. Their IMS locations are shown on this map using labels corresponding to each group. Their IMS local magnitudes range from 0.22 to 2.6. Even though IMS locations gave a good idea of the event locations, they were not accurate enough to distinguish between events from two mines 5 km apart.

Table 2: One-hundred-forty-four events recorded at FINESA.

Ref.	V.	C.	H.C.	Date	Time	ml	Lat1	Lon1	Lat2	Lon2
c93	#	Z2	AU	04/24/91	10:00:33	1.49	61.81	30.78	59.27	27.69
c7	#	Z1	HB9	11/21/90	12:17:07	1.26	60.71	28.50	59.2	27.6
c79	#	W	NR	04/09/91	12:57:51	1.08	60.10	28.98	-----	-----
c104	#	Z2	NR	04/29/91	10:59:55	1.49	60.07	30.80	-----	-----
c17	?	B1	NR	12/16/90	02:40:17	1.06	61.92	29.55	-----	-----
c37	?	Z2	NR	01/08/91	19:40:37	0.47	61.87	29.79	-----	-----
c40	?	Z2	NR	01/15/91	10:03:54	0.38	60.89	29.96	-----	-----
c41	?	Z2	NR	01/16/91	00:07:25	0.59	61.87	30.36	-----	-----
c101	?	Z1	NR	04/26/91	11:33:56	0.61	61.34	28.70	-----	-----
c112	?	Z2	NR	05/12/91	12:45:19	0.37	60.11	28.97	-----	-----
c113	?	Z2	NR	05/12/91	13:06:58	0.20	60.07	28.90	-----	-----
c136	?	B1	NR	06/06/91	20:41:54	0.74	61.81	29.63	-----	-----
c144	?	B1	NR	06/28/91	07:31:24	0.59	61.02	29.18	-----	-----
c10	A	A	AU	11/26/90	12:01:35	1.27	60.76	28.76	61.04	28.31
c3	A	A	NR	11/15/90	08:02:47	0.83	60.59	28.83	-----	-----
c30	A	A	NR	01/03/91	12:50:42	0.96	60.68	28.72	-----	-----
c33	A	A	NR	01/04/91	12:37:10	0.94	60.77	28.41	-----	-----
c36	A	A	NR	01/07/91	10:31:23	0.91	60.68	28.80	-----	-----
c45	A	A	NR	01/30/91	12:37:27	0.90	60.57	28.81	-----	-----
c47	A	Z1	NR	02/04/91	12:10:58	0.76	60.77	28.77	-----	-----
c48	A	Z2	NR	02/06/91	12:06:49	0.40	60.79	28.69	-----	-----
c106	A	A	NR	04/30/91	11:03:02	1.00	60.74	28.61	-----	-----
c111	A	A	NR	05/10/91	11:03:20	1.07	60.98	28.31	-----	-----
c34	B	B2	N117	01/04/91	14:17:51	1.37	61.80	29.63	61.9	29.0
c29	B	B1	NR	01/02/91	11:52:31	0.50	61.76	29.81	-----	-----
c31	B	B1	NR	01/03/91	19:37:23	0.66	61.92	29.43	-----	-----
c32	B	B1	NR	01/04/91	11:39:42	0.88	61.74	29.63	-----	-----
c38	B	B1	NR	01/14/91	11:42:44	0.70	61.92	29.80	-----	-----
c39	B	B1	NR	01/14/91	19:50:54	0.71	61.63	29.81	-----	-----
c44	B	B2	NR	01/28/91	14:23:25	1.28	61.68	28.55	-----	-----
c52	B	B1	NR	03/11/91	11:46:43	0.54	61.72	29.52	-----	-----
c54	B	B1	NR	03/11/91	19:40:21	0.56	61.94	29.43	-----	-----
c56	B	B1	NR	03/14/91	11:47:30	1.04	61.73	29.50	-----	-----
c62	B	B1	NR	03/21/91	19:38:48	0.70	61.75	29.68	-----	-----
c67	B	B1	NR	03/26/91	19:39:11	0.68	61.73	29.47	-----	-----
c78	B	B1	NR	04/08/91	21:56:35	0.60	61.76	28.82	-----	-----
c86	B	Z2	NR	04/17/91	18:43:58	0.92	61.86	28.88	-----	-----
c88	B	Z2	NR	04/18/91	18:50:56	0.37	61.72	29.66	-----	-----
c92	B	B1	NR	04/22/91	18:50:23	0.54	61.57	29.67	-----	-----
c109	B	B1	NR	05/08/91	18:37:51	0.25	61.76	29.26	-----	-----
c116	B	B1	NR	05/14/91	18:40:40	0.37	61.78	29.51	-----	-----
c122	B	B1	NR	05/23/91	19:33:23	0.47	61.44	29.61	-----	-----
c126	B	Z2	NR	05/29/91	20:51:57	0.38	61.75	29.69	-----	-----
c133	B	B1	NR	06/04/91	18:55:28	0.22	61.76	29.48	-----	-----

Table 2: One-hundred-forty-four events recorded at FINESA.

Ref.	V.	C.	H.C.	Date	Time	ml	Lat1	Lon1	Lat2	Lon2
c18	C	C	HC4	12/17/90	12:51:58	1.96	60.76	29.09	60.8	29.3
c81	C	C	HC5	04/11/91	13:21:38	2.14	60.93	28.94	60.9	29.3
c140	C	C	HC5	06/26/91	12:31:59	2.09	60.93	29.01	60.9	29.3
c12	C	C	HC6	11/29/90	12:29:11	2.66	60.91	29.13	60.9	29.4
c69	C	C	HC6	03/28/91	14:49:15	2.32	60.90	28.96	60.9	29.4
c123	D	D	AU	05/24/91	12:02:00	1.99	60.80	28.96	60.92	29.03
c49	D	D	HC6	12/14/90	11:52:05	2.22	61.11	29.15	60.9	29.4
c77	D	D	HC6	04/08/91	11:41:08	1.76	60.98	28.97	60.9	29.4
c53	E	E	AU	03/11/91	12:29:45	2.12	60.91	29.02	60.95	29.03
c94	E	E	AU	04/24/91	12:07:05	2.25	60.98	29.08	60.96	29.30
c98	E	E	AU	04/25/91	12:10:27	2.18	60.89	29.13	61.00	29.17
c129	E	E	AU	05/31/91	13:55:23	2.18	61.03	29.11	60.89	29.12
c22	E	E	HC5	12/25/90	12:28:48	2.16	60.78	29.08	60.9	29.3
c28	E	E	HC5	12/28/90	12:27:34	2.08	60.95	29.10	60.9	29.3
c89	F	F	HC4	04/19/91	12:43:01	1.76	60.93	29.12	60.8	29.3
c21	F	F	HC5	12/22/90	16:48:34	1.99	60.75	29.08	60.9	29.3
c134	F	F	HC5	06/05/91	11:43:12	1.79	60.77	29.01	60.9	29.3
c2	G	G	HC2	11/05/90	12:00:21	2.13	60.85	29.05	60.7	29.0
c50	G	G	HC2	03/07/91	11:11:24	2.29	60.64	28.72	60.7	29.0
c97	H	.	AU	04/25/91	10:43:00	2.05	60.75	29.03	60.67	29.07
c117	H	H	AU	05/21/91	12:33:30	1.86	60.78	29.05	60.74	28.99
c125	H	H	AU	05/29/91	14:06:55	1.85	60.74	28.73	60.64	28.96
c57	H	H	HC1	03/14/91	11:08:08	1.73	60.72	28.91	60.7	28.7
c11	H	H	HC2	11/27/90	12:17:01	1.42	60.67	28.55	60.7	29.0
c75	H	H	HC2	04/04/91	12:53:16	1.50	60.75	28.82	60.7	29.0
c16	K	K	AU	12/06/90	14:22:38	2.22	60.85	29.19	60.89	29.09
c46	K	K	AU	01/30/91	12:59:33	2.24	60.85	29.15	60.89	29.11
c74	K	K	AU	04/03/91	12:25:23	1.99	60.94	29.11	60.91	29.16
c76	K	K	AU	04/05/91	12:54:23	2.14	60.91	29.13	60.92	29.13
c95	K	K	AU	04/24/91	13:10:52	2.32	60.84	29.04	60.90	29.21
c27	K	K	HC4	12/27/90	12:30:36	2.23	60.83	29.23	60.8	29.3
c51	K	K	HC6	03/07/91	12:37:41	2.17	60.78	29.24	60.9	29.4
c142	K	K	HC6	06/27/91	13:08:04	2.40	60.87	29.12	60.9	29.4
c35	L	L	AU	01/05/91	11:41:24	1.56	60.91	29.64	60.90	29.31
c25	M	K	AU	12/26/90	10:07:28	2.25	60.83	29.31	60.83	29.21
c9	M	M	HC5	11/24/90	07:48:19	1.65	60.89	29.43	60.9	29.3
c85	M	M	HC6	04/17/91	09:48:32	1.94	60.97	29.17	60.9	29.4
c60	M	K	HC7	03/20/91	11:59:51	1.93	60.96	29.19	60.8	29.5
c82	M	M	HC7	04/12/91	14:23:49	1.68	60.97	29.15	60.8	29.5
c132	M	M	NR	06/04/91	12:00:02	1.11	61.07	29.35	-----	-----
c108	O	O1	AU	05/06/91	16:07:34	2.06	60.55	29.40	60.48	29.19
c124	O	O2	AU	05/28/91	16:13:45	1.87	60.53	29.25	60.51	29.09
c23	O	O1	HC1	12/25/90	14:50:11	1.25	60.44	29.31	60.7	28.7
c73	O	O2	HC3	04/02/91	14:14:26	2.01	60.64	28.95	60.6	29.2

Table 2: One-hundred-forty-four events recorded at FINESA.

Ref.	V.	C.	H.C.	Date	Time	ml	Lat1	Lon1	Lat2	Lon2
c4	O	O1	NR	11/16/90	12:51:27	1.54	60.56	29.03	-----	-----
c100	O	O2	NR	04/25/91	13:08:04	1.67	60.54	29.24	-----	-----
c121	P	P	AU	05/23/91	13:29:58	1.68	61.21	29.97	61.07	30.03
c128	P	P	AU	05/31/91	13:33:41	1.43	61.15	29.88	61.10	29.88
c8	P	P	HC10	11/22/90	11:37:10	1.88	61.24	29.95	61.1	29.9
c14	P	P	HC10	11/30/90	11:49:14	1.48	61.03	29.94	61.1	29.9
c59	P	P	HC10	03/19/91	16:16:40	1.67	61.17	29.69	61.1	29.9
c66	P	P	HC10	03/25/91	09:23:51	2.06	61.21	29.78	61.1	29.9
c72	P	P	HC10	04/02/91	09:48:18	1.68	61.13	30.11	61.1	29.9
c90	P	P	HC10	04/19/91	12:58:09	1.93	61.17	29.85	61.1	29.9
c87	P	P	HC11	04/18/91	13:14:26	1.59	61.40	29.79	61.1	30.2
c135	P	P	HC11	06/05/91	14:26:01	1.27	60.91	29.54	61.1	30.2
c68	P	P	NR	03/28/91	09:19:48	1.53	61.27	29.82	-----	-----
c105	P	P	NR	04/30/91	10:57:16	1.59	61.30	29.83	-----	-----
c99	R	R	AU	04/25/91	12:42:54	1.89	61.85	30.40	61.86	30.66
c5	R	R	HC13	11/16/90	13:01:22	2.31	61.92	30.44	61.9	30.6
c13	R	R	HC13	11/30/90	09:50:22	1.43	61.93	30.50	61.9	30.6
c19	R	R	HC13	12/18/90	08:59:28	1.28	61.88	30.43	61.9	30.6
c20	R	R	HC13	12/19/90	11:01:31	2.05	62.00	30.38	61.9	30.6
c42	R	R	HC13	01/21/91	10:00:47	1.46	61.78	30.38	61.9	30.6
c71	R	R	HC13	03/29/91	13:41:28	1.89	61.96	30.28	61.9	30.6
c80	R	R	HC13	04/10/91	10:10:09	1.04	61.88	30.31	61.9	30.6
c84	R	R	HC13	04/17/91	08:46:47	1.26	61.86	30.45	61.9	30.6
c114	R	R	HC13	05/13/91	08:52:24	1.08	61.69	30.35	61.9	30.6
c61	R	R	NR	03/21/91	08:08:54	0.85	61.86	30.17	-----	-----
c26	S	S	AU	12/27/90	10:36:59	2.54	61.80	30.59	61.75	30.79
c43	S	S	AU	01/25/91	12:20:30	2.12	61.94	30.44	61.86	30.66
c83	S	S	AU	04/13/91	11:52:34	2.55	61.81	30.66	61.71	30.92
c65	S	S	HC13	03/23/91	12:07:26	2.45	61.84	30.60	61.9	30.6
c110	S	S	NR	05/10/91	07:10:04	1.23	61.91	30.39	-----	-----
c137	T	W	AU	06/07/91	05:39:36	2.32	60.06	29.59	60.11	29.69
c143	T	.	HB15	06/27/91	15:22:31	2.40	60.10	29.61	60.0	29.9
c118	U	Z2	NR	05/23/91	12:09:53	0.78	60.66	30.54	-----	-----
c120	U	Z2	NR	05/23/91	13:27:15	0.75	60.62	30.57	-----	-----
c130	V	S	NR	06/01/91	12:46:19	1.05	60.74	30.49	-----	-----
c131	V	W	NR	06/01/91	13:41:11	1.12	60.82	30.53	-----	-----
c103	W	W	AU	04/26/91	13:28:10	1.56	61.71	31.20	61.31	31.56
c127	W	W	AU	05/31/91	12:55:57	2.31	61.69	31.42	61.52	31.74
c138	W	W	AU	06/07/91	17:47:06	1.47	61.48	31.01	61.66	31.95
c1	W	W	HC14	11/05/90	09:46:23	1.74	61.42	31.55	61.4	31.6
c15	W	W	HC14	11/30/90	15:07:45	2.42	61.61	31.44	61.4	31.6
c24	W	W	HC14	12/26/90	08:47:57	1.82	61.70	31.42	61.4	31.6
c58	W	W	HC14	03/19/91	11:27:01	1.62	61.74	30.86	61.4	31.6
c91	W	W	HC14	04/19/91	13:08:41	1.80	61.67	31.23	61.4	31.6

Table 2: One-hundred-forty-four events recorded at FINESA.

Ref.	V.	C.	H.C.	Date	Time	ml	Lat1	Lon1	Lat2	Lon2
c141	W	W	HC14	06/26/91	13:47:53	2.32	61.84	31.02	61.4	31.6
c55	W	W	NR	03/13/91	10:11:56	0.87	61.88	31.05	-----	-----
c96	W	W	NR	04/25/91	09:38:12	1.09	61.54	30.81	-----	-----
c63	a	K	HC7	03/22/91	13:22:27	1.71	60.80	29.10	60.8	29.5
c70	b	D	HC5	03/29/91	13:38:51	2.37	60.97	28.86	60.9	29.3
c102	d	C	AU	04/26/91	12:13:15	2.04	61.02	28.99	60.99	29.02
c64	h	F	HC5	03/22/91	12:34:16	1.55	60.99	29.07	60.9	29.3
c119	k	K	AU	05/23/91	13:03:18	2.13	60.89	29.22	60.90	29.17
c6	k	O	HC6	11/20/90	13:13:52	1.31	60.79	28.51	60.9	29.4
c107	k	E	NR	05/04/91	14:27:50	0.50	60.86	29.52	-----	-----
c139	m	M	HC6	06/26/91	12:04:19	1.93	60.90	29.17	60.9	29.4
c115	m	D	NR	05/14/91	05:51:45	0.83	61.05	29.14	-----	-----

Ref.: Reference number

V.:Visual classification results

C.:Cluster analysis results

H.C.: Helsinki mine location, (AU:automatic; NR: Not reported in the bulletin)

ml: IMS local magnitude

Lat1, Lon1: IMS coordinates

Lat2, Lon2: Helsinki coordinates

#: events that do not belong to the Karelian mine district

?: events not classified visually because of a low signal-to-noise ratio

.: Multiple event

1.48° (165 km) and 2.65° (295 km) and the azimuthal coverage was 50°. For 89 of the events, a location was reported in the bulletin from Helsinki (monthly or weekly bulletins). In *Figure 5*, locations from the IMS are compared with the locations from the Helsinki bulletin. The average difference in location between events in these two bulletins was 23.01±0.23 km for the manual locations and 24.45±8.30 km for the automatic locations. The large discrepancy between the standard errors of these mislocations is due to four events that were grossly mislocated by the IMS

Results of the visual classification

To do the visual classification, an upper limit on the number of groups was set above which signals were considered to belong to the same group even though small differences could be observed. The number of groups was defined by the results of cluster analysis. All of the events were classified into 18 basic groups. *Figure 6* shows the reference events

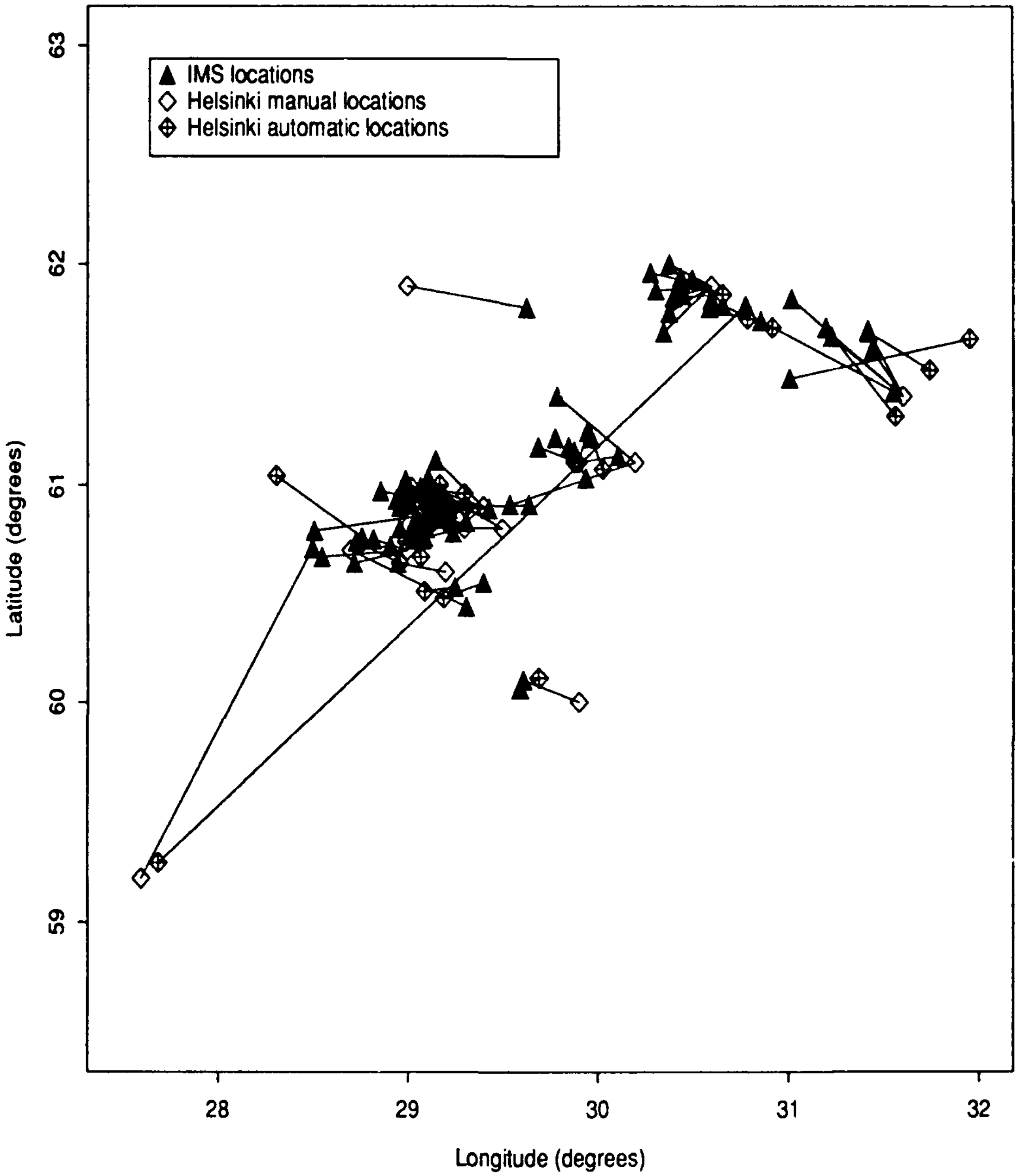

Figure 5: Eighty-nine of the events studied were reported in the Helsinki bulletin; 31 events were located automatically and 55 events had "manual locations". On this plot, IMS locations are compared with Helsinki locations, both manual and automatic. The largest discrepancies in location occur for events with a low signal-to-noise ratio. Two of them were clearly mislocated by the IMS. An interactive *f-k* analysis further confirmed that the azimuths determined by the IMS were erroneous.

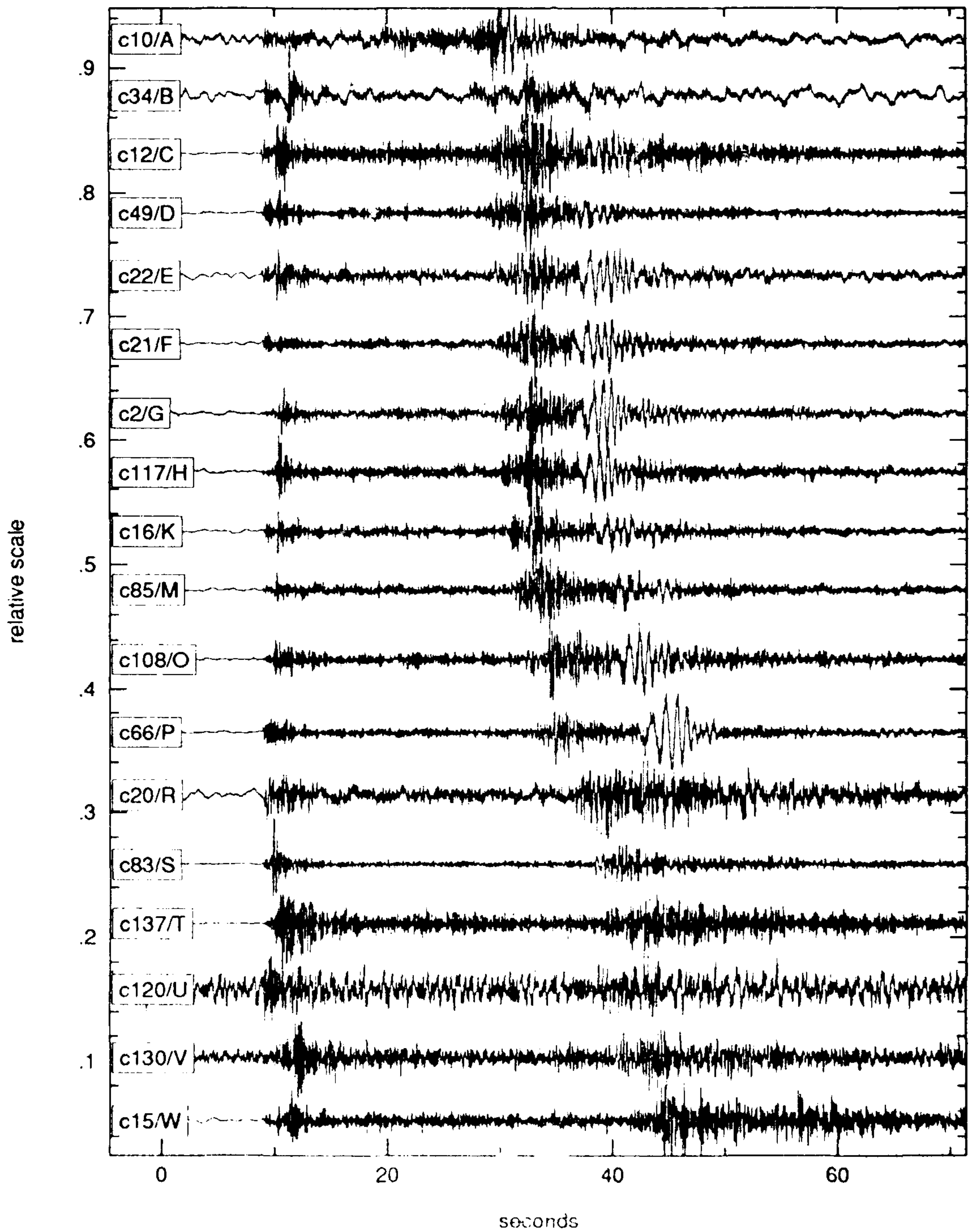

Figure 6: Reference events for 18 groups determined by visual analysis of the data. Both unfiltered and filtered data were used. Groups are labeled from **A** through **W**.

that were identified as representing distinct waveforms. Each group has been labeled with a capital letter that will be used in the text to refer to these groups: **A** being the nearest group to FINESA and **W** being the farthest group. To illustrate the repeatability of these mining events, all the events belonging to groups **K** and **S** are displayed in *Figure 7*.

The events from group **A** were unique: the *Lg* phase was barely observable and the *Rg* phase was strong. For the ten events included in this group, the automatic phase identification of IMS identified only one event with an *Lg* phase. For the remaining nine events, the analyst reviewing the IMS solutions either added an *Lg* or renamed *Rg* to *Lg*.

B was the largest group with 18 events. In addition to having a small *Lg-P* time, their poor signal-to-noise ratio made them unique in the data set. These events were mostly located in Finland according to the IMS and their locations spread over a large area (100 km^2). Because most of the **B** events had a magnitude less than 1.0, only the largest event (c111)

with a magnitude of 1.07 was reported in the Helsinki bulletin

Groups **C** through **M** included events related to a cluster of mines, all within an area of about 16 km^2. This subgroup was the most challenging to the clustering technique. The *Lg-P* time as well as the *Rg-P* time were not characteristic enough to allow a classification based on these parameters. However, the shape of the first *P* arrival along with the shape of the *PMP* phase were used in the visual classification. The first five seconds of the signal for representatives of the eight groups **C** through **M** are plotted in *Figure 8*. The interpretation of results from the cluster analysis made it necessary to distribute these events into ten main groups.

Events from group **O** were easily identified based on their unique *Lg-P* and *Rg-P* times.

The events from group **P** occurred at mines HC10 or HC11 according to the Helsinki bulletin. A thorough visual analysis along with the results of the cluster analysis, showed that their *Lg-P* times were within one second of each other. Only one mine has been located on SPOT photos for this area (SC10).

Events from groups **R** and S, which were all located at mine HC13 according to the Helsinki bulletin, were separated into two groups based on the shape of the first arrival. The difference in the shape of the first arrival could be due either to a difference in the source or to a path effect. **R** events exhibited an impulsive *P* arrival while the **S** events showed an emergent *P* followed by a strong second arrival (probably a *PMP* wave). Even though **R** events had smaller magnitudes, an *f-k* analysis showed that no emergent *P*-wave could be distinguished before the impulsive *P. Figure 9* shows one event from each group with approximately the same magnitude. The *Lg-P* time was slightly larger for the events from S. This observation implies the presence of two mines so close to each other that a regular

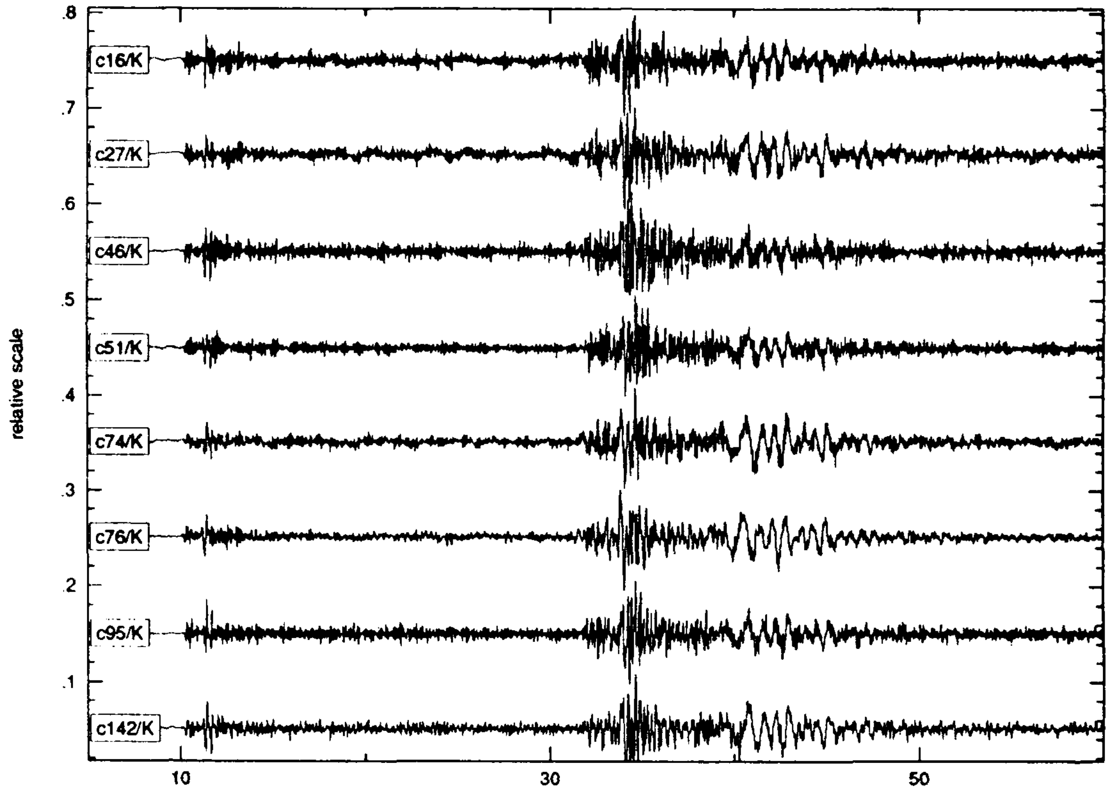

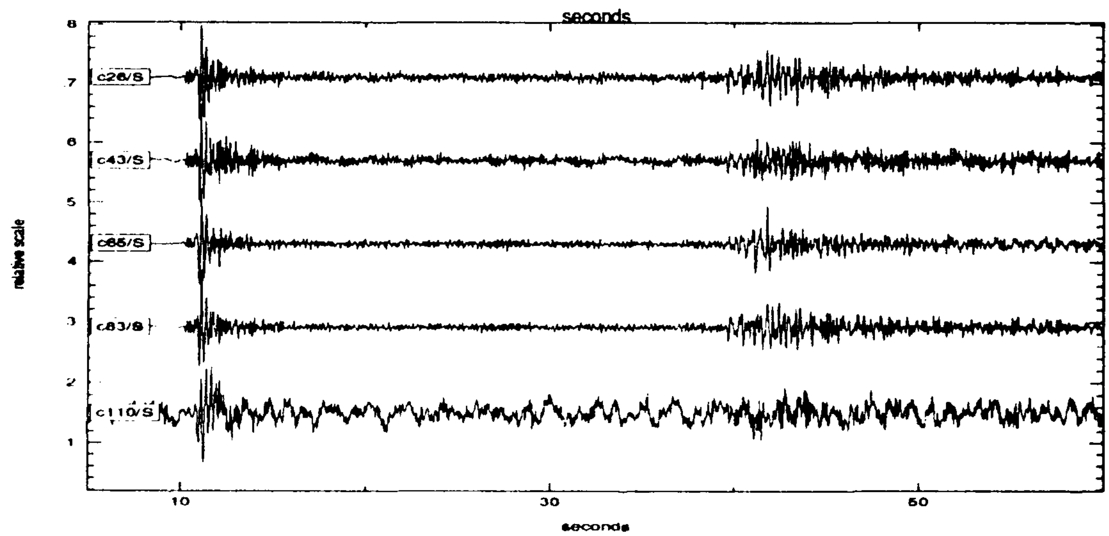

Figure 7: Events from group **K** and **S** are plotted to show the difference between two groups as well as the repeatability of the signal in each group. A difference is clearly seen in the *Lg-P* time and in the presence of an *Rg* phase. For other groups, a difference is evident only in the shape of the first arrival, the *Lg-P* time being the same.

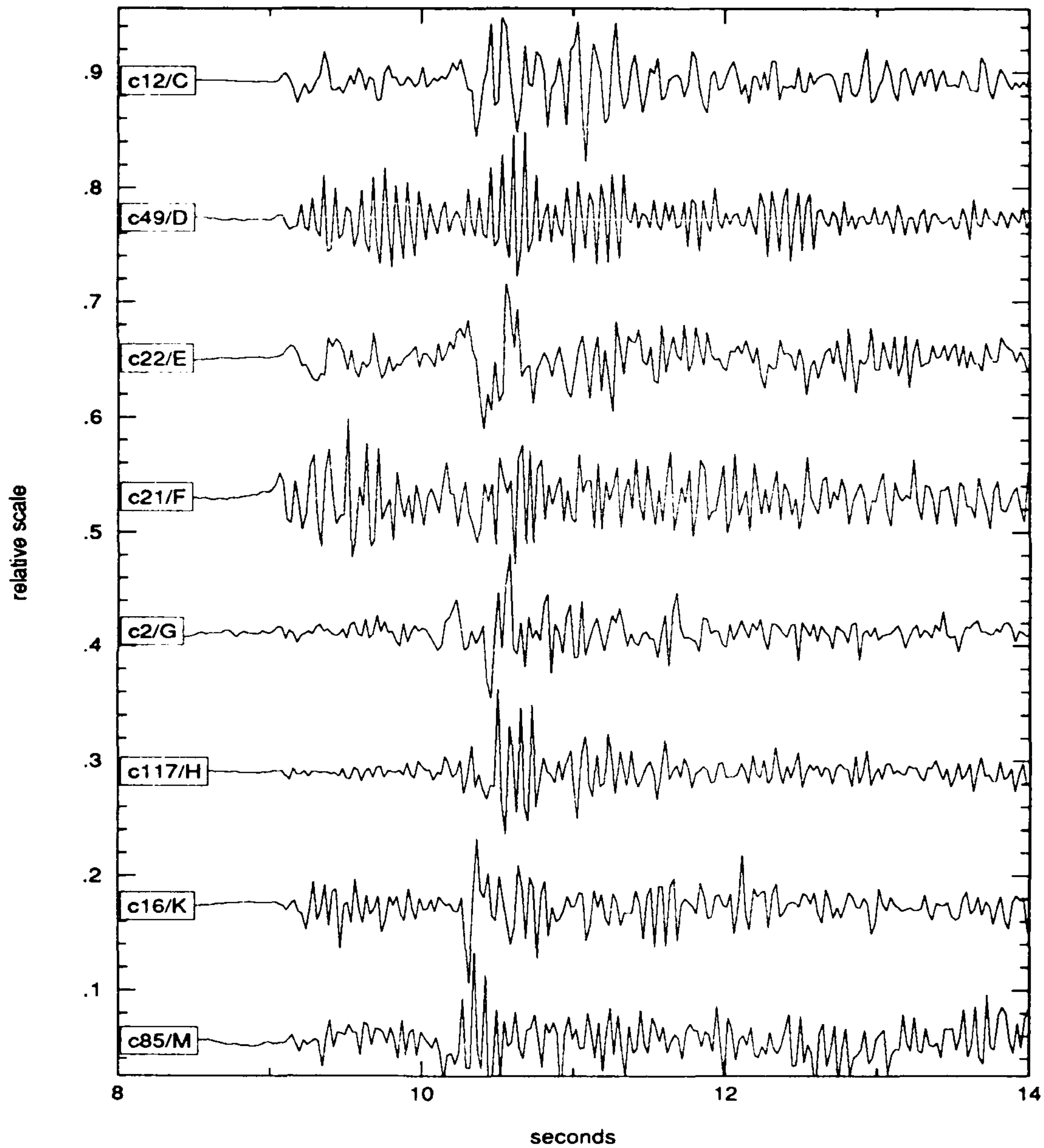

Figure 8: This figure shows the first arrival of reference events for groups **C** through **M**. Their *Lg-P* times and *Rg-P* times vary by less than one second. Differences between events can best be seen using unfiltered data to look at the shape of the first arrival. Although only four mines have been reported in this area in the Helsinki Bulletin, visual classification and cluster analysis determined 8 groups with more than one event and two with only one event. A careful SPOT photo analysis should be performed to determine whether or not this subdivision corresponds to a real distribution of the mines.

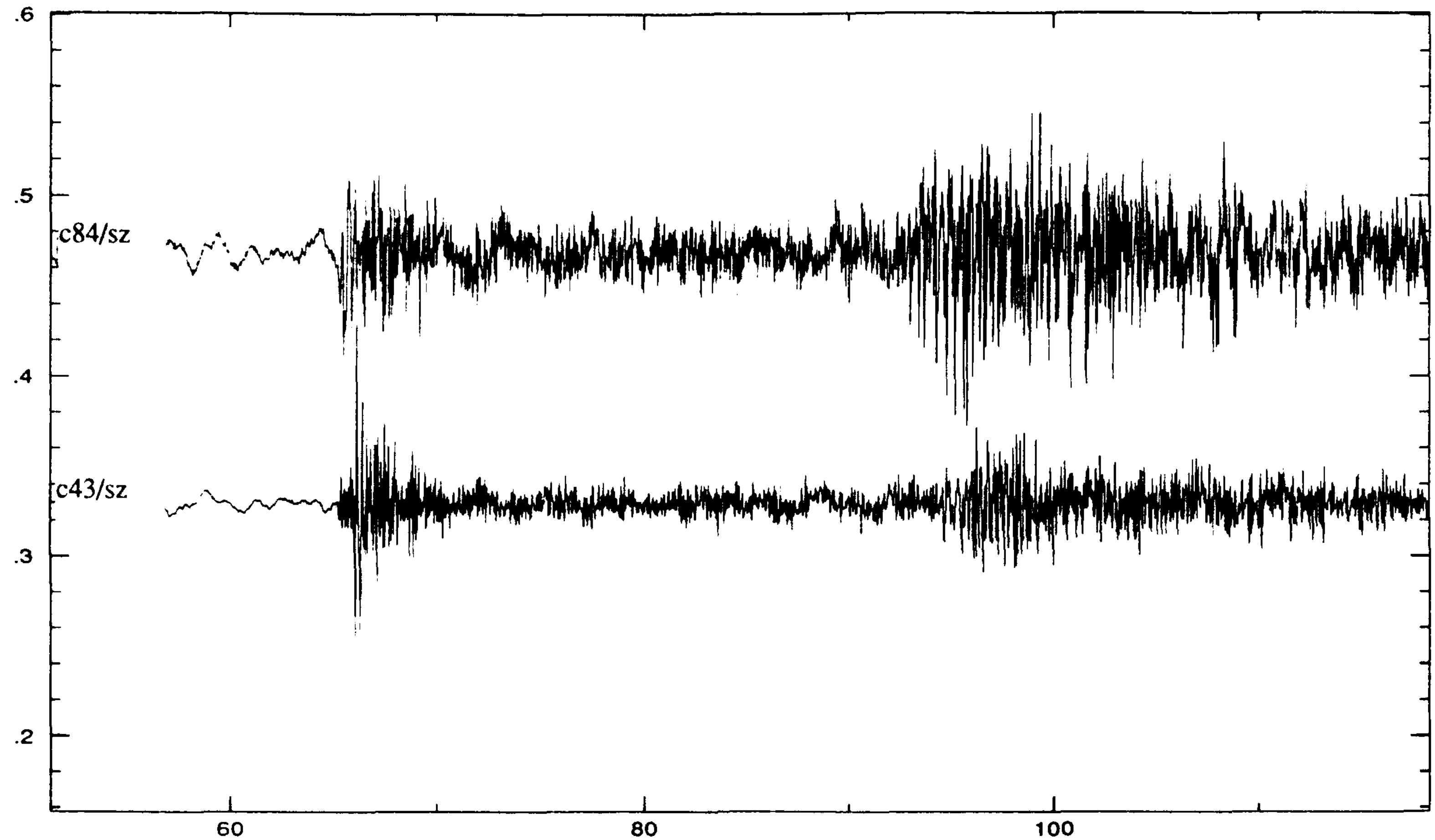

Figure 9: Two events from group **R** and group **S** have been plotted. They have a magnitude of 2.05 and 2.12, respectively. Groups **R** and **S** are located at the same mine according to the Helsinki bulletin (HC13). In the absence of the SPOT photo location for this mine, two assumptions can be made: either these events are from two different parts of the same large mine or they come from the same mine and have different source parameters.

location routine could not distinguish between them. The quality of the SPOT photo presently available for this area did not allow a confirmation or a denial of the presence of two different mines.

Groups U and V contained two events each and were located within 22 km of each other by the IMS but far from any reported mine. They were the only events located in this particular area during the 7-month period. Two events (U) occurred on one day and the other two (V) one week later at about the same time of the day.

The events from group W showed a large scatter in their location despite their relatively high magnitudes. The IMS located most of them close to the SPOT location HC14. Their *Lg-P* time was unique and the *Rg* phase had very small amplitudes for most of the events.

Four events did not fit any of the 18 groups described above. The visual analysis showed that these four events were clearly mislocated by IMS; one event had a *Lg-P* time too large for it to be located within the studied area, and the other three events had very poor IMS azimuth estimates and were actually located in Estonia. These observations were later confirmed by the interactive *f-k* analysis as discussed below.

Some conclusions based on the visual classification are given below:

- Most of the groups were easily distinguished using their *Lg-P* and *Rg-P* time.
- For groups C through M, the shape of the first arrival was a determining factor.
- The visual review showed that four events were mislocated in the IMS bulletin.
- The *Rg* phase was an important feature among the characteristics used to separate different groups. It has been shown that *Rg* waves are strongly site dependent (Murphy and Shah, 1988).
- The resulting visual classification agreed partially with the Helsinki "manual location" but more groups were found than the number of mines reported in the Helsinki bulletin.

Results of the interactive f-k analysis

A *f-k* analysis was performed on each event using a 0.5 s window starting at the beginning of the first arrival. Table 3 shows the average values and standard deviations of the apparent velocity and the azimuth (Aziml, Ap. vell) computed for each group. The average values included only the events for which the visual classification was in agreement with the cluster analysis. Only eight events belonging to group B were studied due to low signal-to-noise ratios. Although these events also had very low signal-to-noise ratios, the values computed with the *f-k* analysis were stable (small standard deviation). The velocities derived from the *f-k* analysis for the first arrival are plotted on a map (*Figure 10*) to show

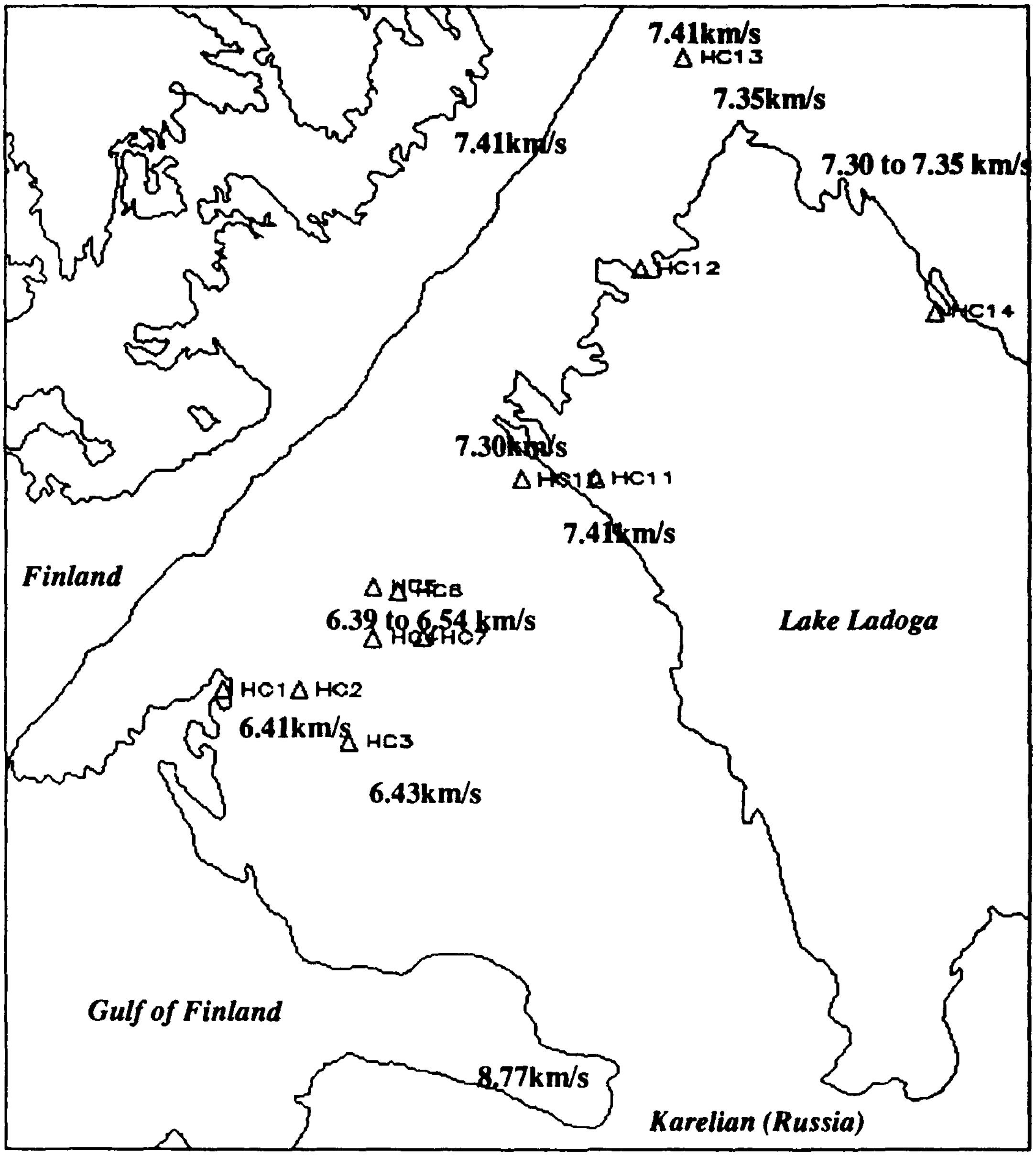

Figure 10: Apparent velocities of the first arrival have been computed for each event using an *f-k* analysis method. This map shows the spatial distribution of the average apparent velocity for each mine group. North of Lake Ladoga, the velocity is around 6.45 km/s while South of the lake, the velocity is around 7.35 km/s and keeps increasing up to 8.77 km/s for the events located on an island in the Gulf of Finland. Strong variations in the thickness of the crust as well as sharp lateral boundaries in the crust can explain these changes in the apparent velocity.

Table 3: Azimuth and velocity values computed automatically by the IMS (Azim2, Ap.vel2) and the same values computed using *f-k* analysis (Azim1, Ap.vel1).

group	Azim1	Ap.vel1	Azim2	Ap.vel2
A	121.27 0.23	6.45 0.04	122.24 3.49	6.77 0.69
B	79.32 0.53	7.42 0.07	78.93 8.55	8.10 0.70
C	120.71 0.36	6.47 0.06	112.99 1.45	7.02 0.09
D	120.68 0.35	6.44 0.09	117.59 2.06	6.76 0.04
E	117.58 7.87	6.65 0.40	111.18 2.14	7.11 0.08
F	120.70 0.86	6.44 0.02	111.73 1.28	6.94 0.15
G	121.05 0.00	6.41 0.00	120.04 0.47	7.12 0.12
H	120.79 0.38	6.43 0.02	119.33 2.64	6.97 0.15
K	120.81 0.55	6.46 0.08	114.16 1.05	7.26 0.09
M	120.72 0.50	6.45 0.04	112.49 1.23	7.10 0.45
O	120.63 0.47	6.43 0.02	122.46 2.65	7.24 0.41
P	102.02 0.68	7.35 0.08	106.20 6.05	7.01 0.28
R	79.43 0.50	7.36 0.06	76.22 1 1.62	6.94 1.06
S	93.52 1.95	7.17 0.38	81.74 10.63	7.39 0.21
U	101.54 0.00	7.46 0.00	106.97 3.47	6.97 0.01
W	101.93 0.97	7.30 0.00	95.01 8.52	7.28 0.42
c7	125.22	6.70	148.24	7.30
c79	134.77	7.19	134.13	8.92
c93	74.44	6.52	168.51	7.46
c104	117.11	8.83	31.39	6.49

their spacial distribution. These events were located at distances from FINESA that correspond to the cross-over point of the travel-time curves for this area. Events located near the northern part of Lake Ladoga showed an apparent velocity ranging between 7.27 to 7.41 km/s; events located south of the lake exhibited an apparent velocity between 6.39 and 6.54 km/s; and events located further south in the Gulf of Finland (Island not plotted on the map) showed an apparent velocity close to 9.0 km/s. The apparent velocity of the second *P* type arrival was about the same for all of the events: 6.5 km/s. The events with the lowest velocity were also the closest to the array and the first arrival was a *Pg* phase. The two other sets of events were at about the same distance from FINESA and the difference in the apparent velocity could be explained by a difference in the travel path. In both cases, the first arrival was a *Pn* phase. However, the crust thickens rapidly from the Gulf of Finland to the Baltic Shield *(Figure 11)*, thus increasing the apparent velocity.

A second *P* phase was seen, more or less clearly, within the two seconds following the first arrival on most of the signals. The second arrival was a *PMP* phase (reflected from the Moho). The presence of this phase was not related to the size of the shot. It did not appear on the signals from group **P** whose magnitudes were between 1.27 and 2.06 while the

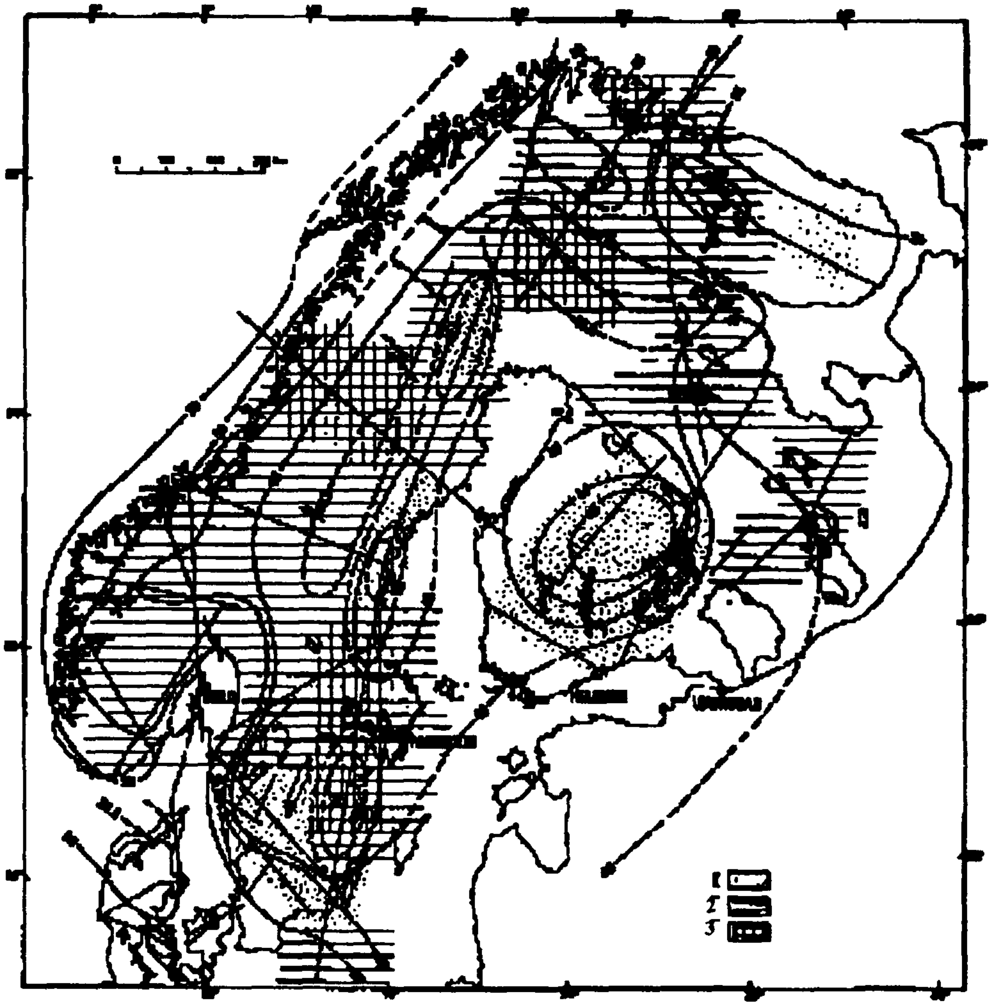

Figure 11: Contour map of crustal thickness (km) and schematic map of *Pn* velocity for the Baltic Shield and adjacent areas based on DSS data. Lines of equal Moho depth are represented by thick solid lines for reliable data and dashed lines for unreliable data. Values of *Pn* velocity are: **1**, 7.8 to 8.0; **2**, 8.1 to 8.3; **3**, 8.3 to 8.5. Thin solid lines denote DSS profiles. The crustal thickness varies from as little as 30 to 35 km near the coast to 50 to 55 km within the interior areas. *Pn* wave velocity varies from 7.8 to 8.0 km/s up to 8.3 to 8.5 km/s (the most frequently observed values are 8.1 to 8.2 km/s). There is no direct relationship between variations of the crustal thickness and *Pn* velocity (Ryaboy, 1990).

events from group **B** with smaller magnitudes (0.22 to 1.37), showed a sharp second arrival. The distance to the array also did not influence it's presence. For instance, events from group **R** did not show the *PMP* phase, but it was seen on signals from groups located both closer to and farther from the array. Lateral heterogeneities, in addition to differences in crustal thickness, may explain the presence of the PMP phase. Its interpretation will require further study.

F-k analysis was performed automatically in the IMS based on a computed arrival time. The window length was 3.0 s and began 1.0 s before the arrival time. Our results were based on a 0.5 s window length, but tests showed that there were no significant differences in the results for window lengths up to 5.0 s. Average values of the apparent velocity and the azimuth computed from the IMS values are reported in Table 3. Only the IMS results for the first arrival are shown and compared to the interactive *f-k* analysis. IMS also stores the results for secondary phases.

A careful *f-k* analysis provides important information about events. Even though computed values for the same group of events are very stable, the azimuth can vary by up to one degree around this value. For our purpose, this is too large of a location error (about 5 km) and the visual classification, if associated with a known mine, provides more accurate results.

Cluster analysis results using waveforms

Figure 12 shows the cluster tree resulting from the analysis of filtered data (1-15 Hz). The lowest level of the tree (cross-correlation value of 0.4) shows the separation between events located north of Lake Ladoga and events located south of the lake. For the branch on the left, there is a dichotomy in the tree separating events with a large *Rg* phase from events with little to no *Rg* phase. At the level of the tree corresponding to a cross-correlation value of 0.57, the cluster separates the events into 10 groups. At this level, groups **A**, **M**, **P**, **R**, **S**, **V** and **W** are defined while events from group **B** are split into two subgroups (**B1** and **B2**) and events from groups **C** through **M** belong to one large group.

The events from group **B** had the smallest signal-to-noise ratios. **B1** corresponds to the largest events with a magnitude greater than 1.0 while the other events group in **B2**. If a narrower frequency band is used (1.0 to 8.0 Hz), no subgroups are obtained.

The **Z** branch of the cluster tree does not define a group of events that look alike. These events cannot be classified in any group because of low signal-to-noise ratio, uniqueness, or the fact that they are multiple events.

Figure 13 shows the cluster tree using the 55 events from groups **C** through **O**. Seven

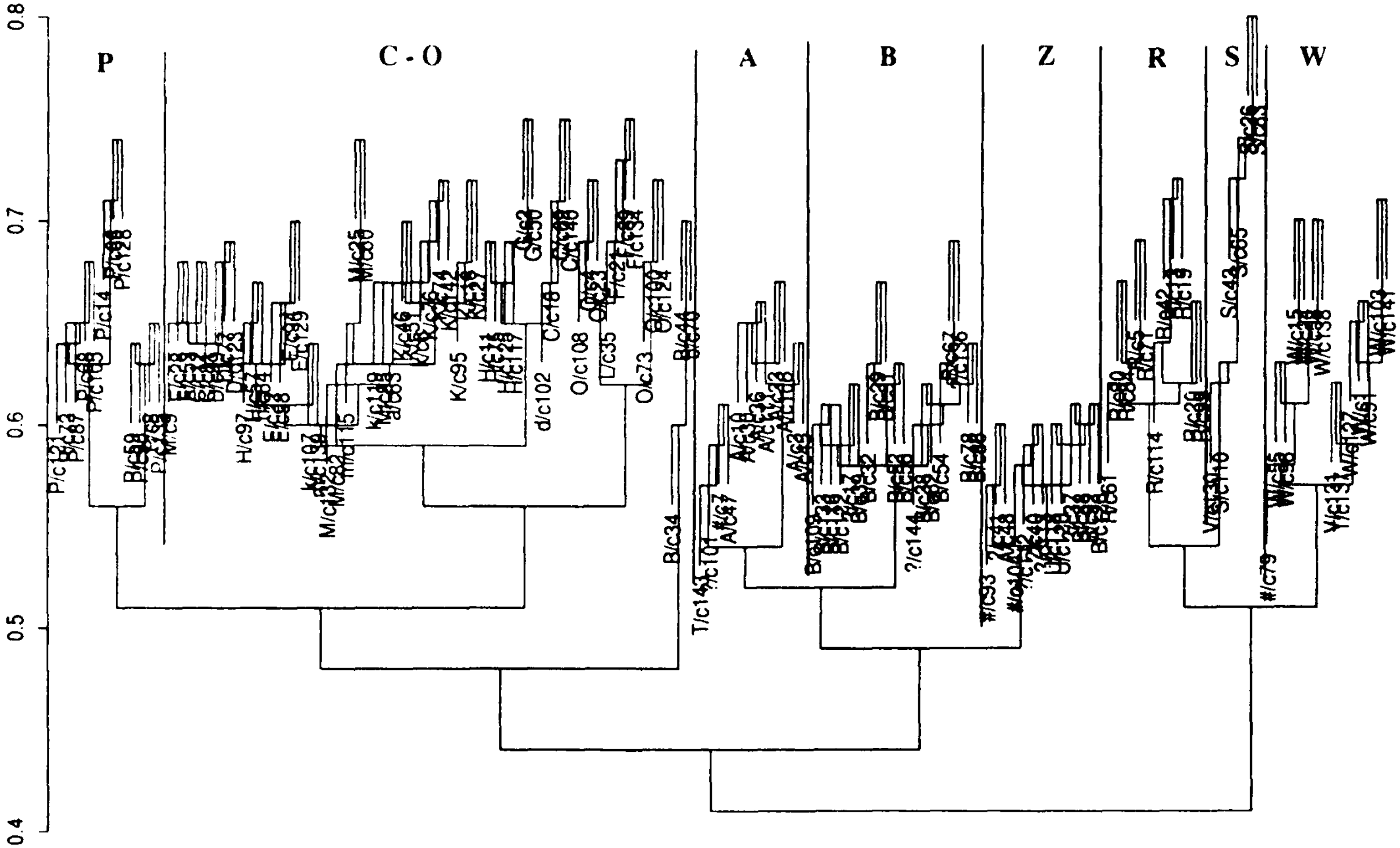

Figure 12: The tree resulting from cluster analysis using a "complete linkage method". Envelopes of filtered data (1-15 Hz) recorded on the vertical channel of the FIA1 sensor were computed. A cross-correlation value was calculated for each pair of events. These cross-correlation values were used as similarity measurements in the cluster analysis.

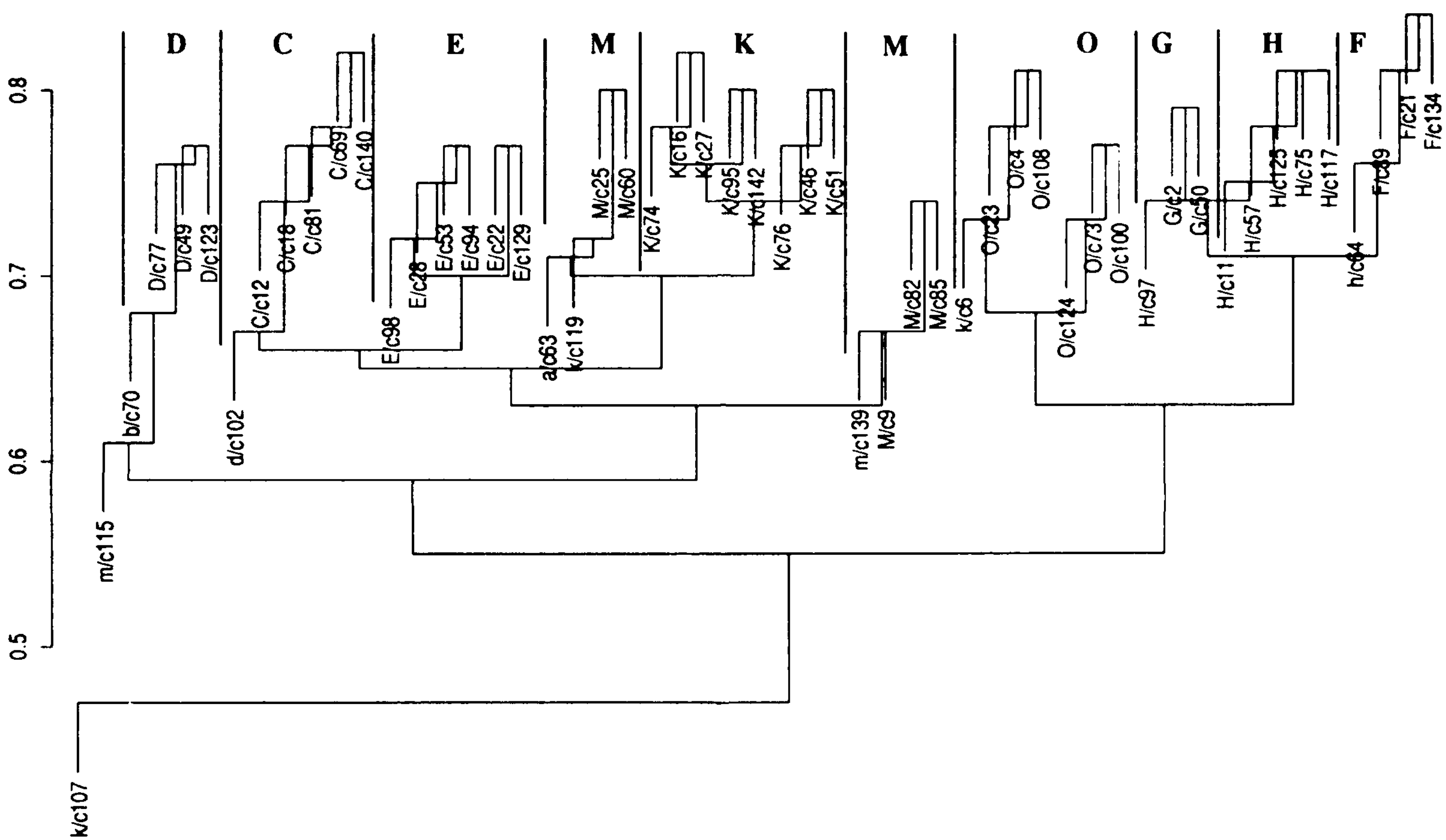

Figure 13: Fifty-three events belonging to groups **C** through **O** have been reprocessed using the frequency band 1-15 Hz. The resulting clustering shows a good agreement with the visual classification. This set of data is especially difficult and in addition to the labels **C ... O**, others labels were used. Lower case letters were used to label events that were similar but not identical to the group labeled with the upper case letter, the difference residing mostly in the *Lg-P* time. The "**a**" label was used for an event that was visually not close to any other group.

small groups can be distinguished from one another at a cross-correlation value of 0.67, but a level of 0.75 must be used to distinguish between groups **F**, **G**, and **H**. The high level of correlation is related to the stability of the shape of the signal in this tight grouping of events. Note that the **M** events, previously grouped together by the visual classification, have been split into two groups here.

The visual classification differed from the cluster analysis for ten of the 144 events without including the events that were labeled with lower case letters. These ten events were characterized either by a low signal-to-noise ratio or were multiple events. Nine events had such a low signal-to-noise ratio that a visual classification could not be performed. The events labeled with lower case letters were unique and could not be classified in any group, thus their visual classification was questionable.

Four events were erroneously included in the data set due to large azimuth errors in the IMS and actually belong to mining districts in other areas. This error was discovered through interactive *f-k* analysis. The *P - Lg* time for these three events was nearly identical to the *P - Lg* time for mines in the study area. One of these events erroneously clustered with events from group **W** while the three other events were classified with either group **Z1** or **Z2**. These events clustered at low levels with events most similar to them.

Cluster analysis results using phase parameters data

The use of *f-k* parameters in addition to other measurements (SNR, period, azimuth, slowness, etc.) computed during the automatic processing of the IMS in a cluster analysis gives results comparable to those that would be obtained by grouping events based on IMS locations. The addition of polarization parameters from three-component polarization analysis did not improve the results of this cluster analysis because polarization parameters are more characteristic of the receiver than of the source.

RESULTS OF THE CLUSTER ANALYSIS USING ARCESS AND NORESS DATA

Among the 144 events, 39 were recorded at ARCESS and 31 at NORESS. Both arrays are located at a distance of about 9° from the mining district. Despite their relatively high magnitudes (1.56 to 2.66 for ARCESS data and 2.01 to 2.66 for NORESS data), the data had low signal-to-noise ratios (*Figure 14*). Envelopes were computed using data filtered between 2.0 and 5.0 Hz. The signal length used in the cross-correlation process was set to 175 s including 15 s before the arrival. The cluster analysis based on these data gave poor

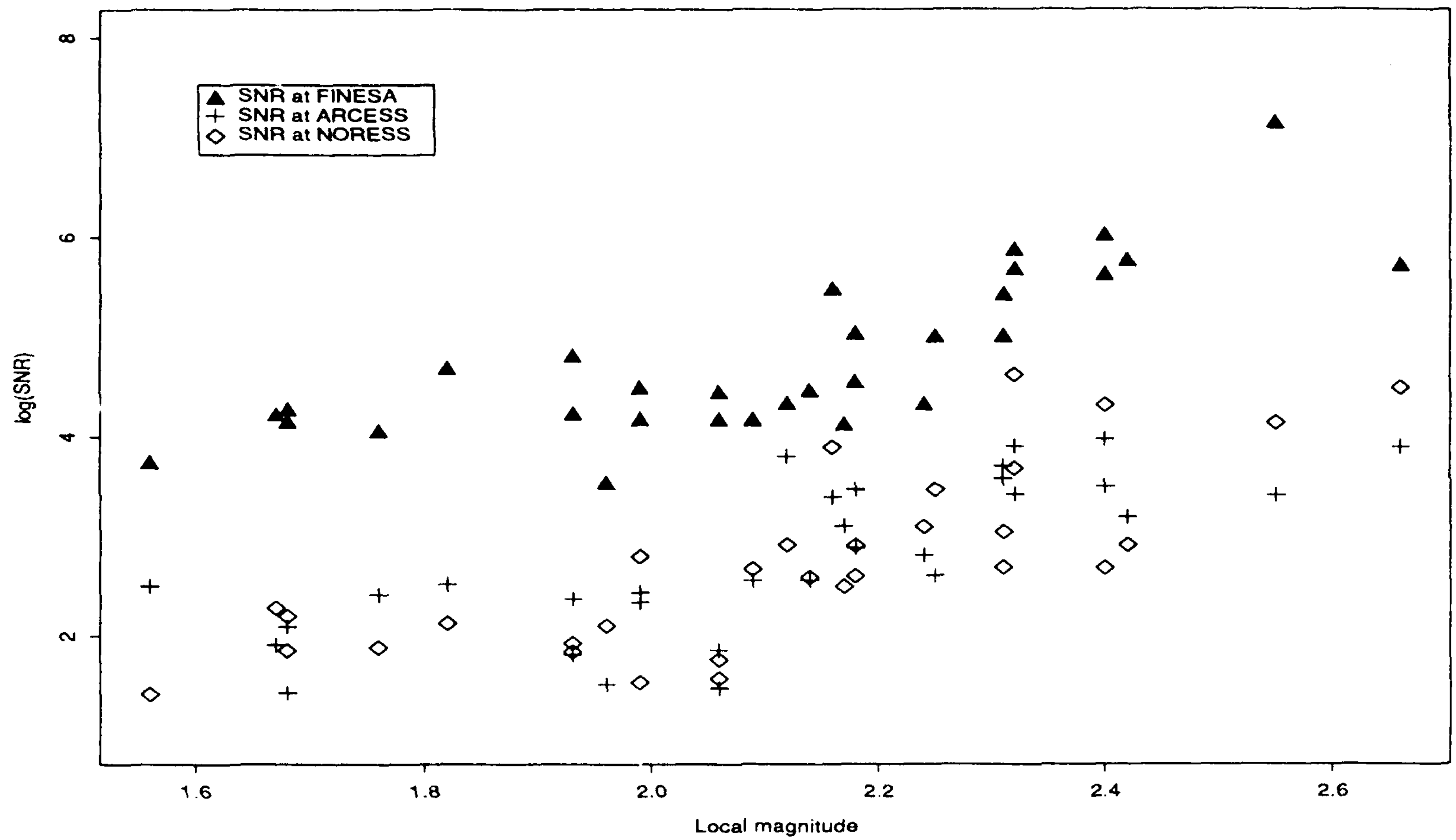

Figure 14: Signal-to-noise ratios are compared for 39 events recorded at the three arrays: ARCESS, NORESS and FINESA. ARCESS and NORESS have very similar values. These two arrays are located at about the same distance from the mining district. The signals recorded at FINESA have a signal-to-noise ratio roughly 9 times higher than the signals recorded at NORESS and ARCESS.

quality results (*Figure 15* and *16*) probably due to poor signal-to-noise ratios and the lack of an *Rg* phase in the NORESS and ARCESS data.

ASSOCIATION OF EVENTS TO MINE LOCATION

Having defined clusters of events both visually and through cluster analysis, the task

becomes associating a mine with each group of events. Twenty-one groups of events were identified above, but only fifteen mines have been listed in the Helsinki Bulletin and even fewer were located on SPOT photos by Fox (1990). Because ground truth was not available for the events used at the time this study was made, seismic locations reported in the IMS and Helsinki Bulletins and the results of the interactive *f-k* analysis was the only information used to make the association. Other information (possibly provided by mining authorities) may be used in future analysis efforts.

Events from group **A** and from group **I** were all located close to mine SC1 (HC1) by the IMS. The visual analysis showed a clear difference in *Lg-P* times between the two groups, however: events from group **I** have *Lg-P* times 8 s greater than the events from group **A**. The Helsinki bulletin reported an automatic location for event c10 from group **A** that was

close to mine N114. The Helsinki bulletin also reported a manual location for event c57 from group **I** at mine HC1. This discrepancy between bulletins may be explained by a misidentification of the phases for group **A** in the IMS. As noted in the visual description of events from group **A**, the analyst often renamed the *Rg* as an *Lg* resulting in a location too far from the array. The distance between HC1 and N114 is 43 km, which corresponds to a difference in travel-time of about 8.25 s. Event c111 with the only *Lg* correctly identified by the IMS for this group of events was located near mine N114. Thus, events from group **A** are associated with mine N114, and events from group **I** are associated with mine SC1 (HC1)

Only one event from group **B** was manually located by the Helsinki analysts. In Table 1, this mine is labeled N117. The interactive *f-k* analysis gave stable values for the events in this group and most of them could be located at this mine. The large scatter observed in the IMS locations for these events is explained by their small magnitudes.

Events from group **O** were located by the IMS close to mine SC3. There was little scatter in the locations. One of these events was manually located at mine HC3 by the Helsinki analysts.

Events from group **P** were located at one of two different mines, HC10 or HC11, accord-

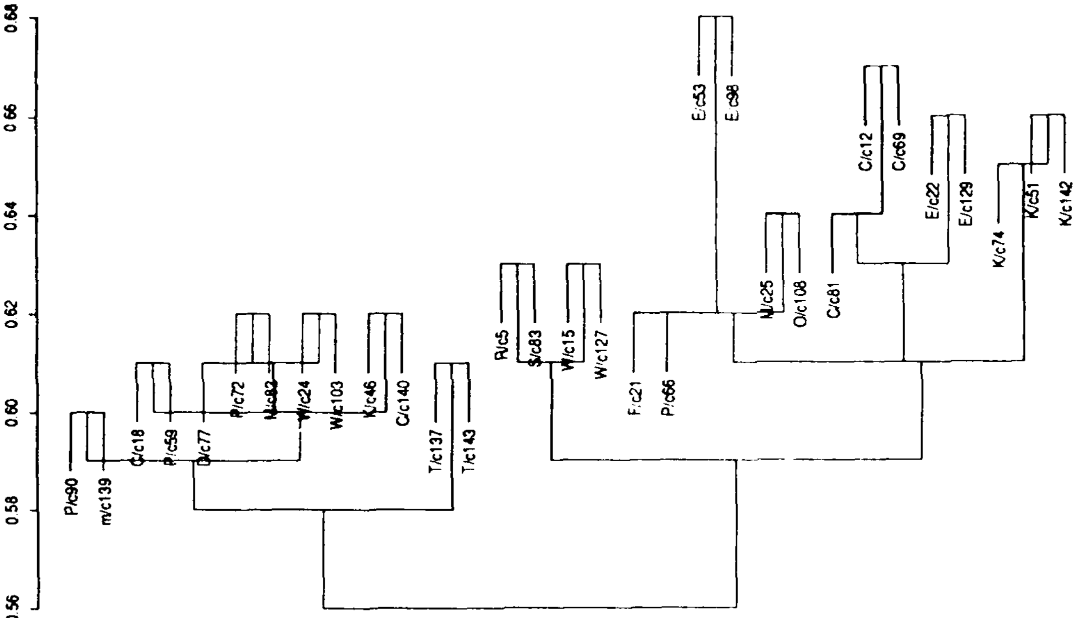

Figure 15: Result of the cluster analysis performed on 31 events recorded at ARCESS. Data were filtered between 2 to 5 Hz. Events with the highest signal-to-noise ratio give reasonable results.

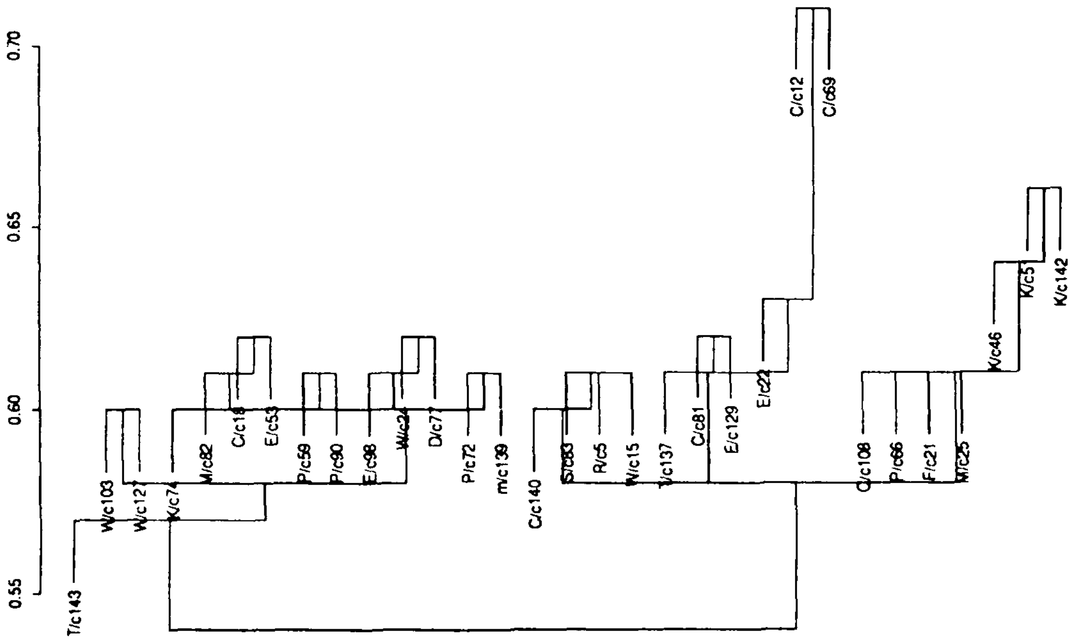

Figure 15: Result of the cluster analysis performed on 31 events recorded at NORESS. The same frequency band applied to the ARCESS data was applied to these signals.

ing to the Helsinki bulletin. For this area, only one mine was reported on SPOT photos by Fox (1990). *Lg-P* times for this group vary by 1.0 s, which is not enough to justify the distance between HC10 and HC11, but could correspond to events from different parts of the same big mine.

Seven events from group **R** and one event from group **S** were manually associated with mine HC13 according to the Helsinki bulletin. Three other events from group S were automatically located around this mine by the same bulletin. Any difference in location

between the two groups was not clearly seen using the IMS location. No reliable SPOT photo was available for this area. Events from groups **R** and **S** may have been from the same large mine or from two different mines.

Events from group **T** were located on an island in the Gulf of Finland where a mine has been identified on a SPOT photo (SB15).

Events from group **U** could not be associated with any mine as none were reported on this part of the southern coast of Lake Ladoga. Although two of the events had an IMS magnitude greater than 1.0, they were not reported in the weekly bulletin from Helsinki. These events may have been related to construction activity.

Events from group **V** were located far from each other by the IMS, probably because of their small magnitude, and they were not reported in the Helsinki bulletin. No mine was

reported close to these events.

The Helsinki bulletin reported five group **W** events and located them all at mine HC14. The IMS locations for the set of events were closer to mine SC14.

Associating the events from groups **C** through **M** with specific mines was not possible with the limited information available. These groups contained events that were located in a small area where only five mines were identified in the Helsinki bulletin and on SPOT photos (SPOT locations can include several small mines). In this particular case, the limitations of the current seismic location procedures are shown. Even when careful *f-k* analysis was used to obtain more stable values of the azimuth, the results were not accurate enough to allow a perfect match between event groups and mines. Possible flaws in the Helsinki manual locations were also observed. In some cases, several events that cluster together and were identified as belonging to the same group visually, were manually located by the Helsinki analysts as originating from different mines.

SUMMARY AND CONCLUSIONS

Events recorded at the FINESA, ARCESS and NORESS arrays were studied with the aim of identifying and characterizing mines located north of St. Petersburg. Both waveforms and parameters computed during the automatic process were used in this study.

Cross-correlation values computed between the envelopes of the vertical component seismograms were found to be the best similarity measurements for use in a cluster analysis. This method was verified by a visual classification of the waveforms along with an interactive *f-k* analysis. The *f-k* analysis provided explanations for the questionable results of the cluster analysis and showed that the assumption of identical travel paths for all of these events was not valid. Eighteen different groups (with more than one event per group) were identified from the 144 events by both cluster analysis and visual classification. Four events were not classified as they were originally mislocated and do not really belong to this mining district.

The Helsinki and IMS bulletins were used as references for the locations of these events. Only 89 events were reported in the Helsinki bulletin for the covered period of time. Fifty-eight events had been "manually located" by the Helsinki analysts at 15 different mines. Their classification agreed with our grouping for events located in areas where only one mine had been reported: HC3, HC10, HC13, HC14 and HB15.

SPOT photos from this area are currently being analyzed. They provide information about the size and the actual number of active mines. This information allows a better classification of the events as the number of groups (mines) is predetermined. But, in order to improve the matching between groups of events and mines, information concerning the origin time, the "true" location of the shot, as well as the shooting parameters and the yield of the shot need to be gathered directly from the mines.

Two other mining districts showing a high concentration of mines are available to test this method. The implementation of this method in an automatic system such IMS would required a selection of master events for each mine. A "pre-location" of a given event by the automatic routine would determine what mining district was relevant. The event would be compared to the reference events built for this particular district. The maximum value of the cross-correlation of the envelope functions would be compared to the thresholds previously determined for each mine by cluster analysis. As seen above, a threshold needs to be set in order to delimit the different groups. If this threshold is too low to separate several groups, a second comparison should be performed using a smaller set of reference events. For mislocated events, the result of the cross-correlation with the master events should give a value below the threshold. In such cases, these events would be re-analyzed carefully.

ACKNOWLEDGEMENTS

The program (massproc) used to compute cross-correlation values directly from the database was written by John Coyne, SAIC. The program (geotool) used for all waveform comparisons, stacking, and *f-k* analysis was written and customized by Ivan Henson, Teledyne Geotech with assistance from John Coyne of SAIC. Information about SPOT photos was provided by Warren Fox, SAIC. The authors would like to thank Jerry Carter for his constant encouragement.

REFERENCES

Bache T.C., J.T. Anderson, D. Baumgardt, S.R. Bratt, W.E. Farrell, R.F. Fung, J.W. Given, A.S. Henson, C. Kobryn, H.J. Swanger, J. Wang (1990). Intelligent Array System. *Final Technical Report, October 1990.* SAIC, San Diego.

Baumgardt, D.R. and K. A. Ziegler (1988). Spectral Evidence for Source Multiplicity in Explosions: Application to Regional Discrimination of Earthquakes and Explosions. *Bull. Seism. Soc. Am.* **78**, 5, 1773-1795.

Baumgardt, D.R. (1987). Case-based Reasoning Applied to Regional Seismic Event Characterization, *DARPA/AFGL Seismic Research Symposium*, Harbor House, Nantucket, MA, 15-18 June 1987, 173-178, GL-TR-90-0300, ADA229025.

Bennett, T.J., B.W. Barker, K.L. McLaughlin, J.R. Murphy (1989). Regional Discrimination of Quarry Blasts, Earthquakes and Underground Nuclear Explosions. *S-Cubed Final Report SSS-TR-89-1039,* GL-TR-89-0114. ADA223148

Blandford, R.R. (1982). Seismic Event Discrimination. *Bull. Seism. Soc. Am.* **72**, S69-S87.

Bratt S.R., H.J. Swanger, R.J. Stead, F. Ryall, T.C. Bache (1990). Initial Results from the Intelligent Monitoring System. *Bull. Seism. Soc. Am.* **80b**, 1852-1873.

Dysart, P.S. and J.J. Pulli (1988). Waveform and Spectral Characteristics of Regional Earthquakes and Chemical Explosions Recorded at the NORESS Array. *Technical Report C88-01*. Center for Seismic Studies, Internal Report.

Everitt, B. (1986). Cluster Analysis. *Halsted Press, Division of John Wiley & Sons, New York* (2nd Edition).

Fox, W. (1990). Satellite Imagery of Areas in Northeast Europe. *Internal Report.* SAIC, San Diego.

Israelsson H. (1990). Analysis of High Frequency Data. *Scientific report #1*, GL-TR-90-0299. Center for Seismic Studies, ADA231804.

Israelsson H., and J. Carter (1991). Analysis of High Frequency Seismic Data. *Scientific report #2*, PL-TR-91-2032. Center for Seismic Studies, ADA235579

Murphy, J.R. and H.K. Shah (1988). An Analysis of the Effects of Site Geology on the Characteristics of Near-field Rayleigh Waves.Bull.Seism.Soc.Am. **78**, 1, 64-82.

Pomeroy, P.W., W.J. Best, T.W. McEvilly (1982). Test Ban Treaty Verification with Regional Data - A Review. *Bull. Seism. Soc. Am.* **72**, S89-S129.

Ryaboy, V. (1990). Upper Mantle Structure along a Profile from Oslo (NORESS) to Helsinki to Leningrad, based on Explosion Seismology. *Bull. Seism. Soc. Am.* **80**, 6, 2194-2213.

Smith, A.T. (1989). High-Frequency Seismic Observations and Models of Chemical Explosions: Implications for the Discrimation of Ripple-fired Mining Blasts. *Bull. Seism. Soc. Am.* **79**, 1089-1110.

Uski, M., E. Polkonen, M. Franssila, M.Raime (1990-1991). Seismic Events in Northern Europe. *Ed. H. Korhonen*.Institute of Seismology, University of Helsinki, Helsinki, Finland.

Prof. Thomas Ahrens
Seismological Lab, 252-21
Division of Geological & Planetary Sciences
California Institute of Technology
Pasadena, CA 91125

Prof. Keiiti Aki
Center for Earth Sciences
University of Southern California
University Park
Los Angeles, CA 90089-0741

Prof. Shelton Alexander
Geosciences Department
403 Deike Building
The Pennsylvania State University
University Park, PA 16802

Dr. Ralph Alewine, III
DARPA/NMRO
3701 North Fairfax Drive
Arlington, VA 22203-1714

Prof. Charles B. Archambeau
CIRES
University of Colorado
Boulder, CO 80309

Dr. Thomas C. Bache, Jr.
Science Applications Int'l Corp.
10260 Campus Point Drive
San Diego, CA 92121 (2 copies)

Prof. Muawia Barazangi
Institute for the Study of the Continent
Cornell University
Ithaca, NY 14853

Dr. Jeff Barker
Department of Geological Sciences
State University of New York
at Binghamton
Vestal, NY 13901

Dr. Douglas R. Baumgardt
ENSCO, Inc
5400 Port Royal Road
Springfield, VA 22151-2388

Dr. Susan Beck
Department of Geosciences
Building #77
University of Arizona
Tuscon, AZ 85721

Dr. T.J. Bennett
S-CUBED
A Division of Maxwell Laboratories
11800 Sunrise Valley Drive, Suite 1212
Reston, VA 22091

Dr. Robert Blandford
AFTAC/TT, Center for Seismic Studies
1300 North 17th Street
Suite 1450
Arlington, VA 22209-2308

Dr. G.A. Bollinger
Department of Geological Sciences
Virginia Polytechnical Institute
21044 Derring Hall
Blacksburg, VA 24061

Dr. Stephen Bratt
Center for Seismic Studies
1300 North 17th Street
Suite 1450
Arlington, VA 22209-2308

Dr. Lawrence Burdick
Woodward-Clyde Consultants
566 El Dorado Street
Pasadena, CA 91109-3245

Dr. Robert Burridge
Schlumberger-Doll Research Center
Old Quarry Road
Ridgefield, CT 06877

Dr. Jerry Carter
Center for Seismic Studies
1300 North 17th Street
Suite 1450
Arlington, VA 22209-2308

Dr. Eric Chael
Division 9241
Sandia Laboratory
Albuquerque, NM 87185

Prof. Vernon F. Cormier
Department of Geology & Geophysics
U-45, Room 207
University of Connecticut
Storrs, CT 06268

Prof. Steven Day
Department of Geological Sciences
San Diego State University
San Diego, CA 92182

Marvin Denny
U.S. Department of Energy
Office of Arms Control
Washington, DC 20585

Dr. Zoltan Der
ENSCO, Inc.
5400 Port Royal Road
Springfield, VA 22151-2388

Prof. Adam Dziewonski
Hoffman Laboratory, Harvard University
Dept. of Earth Atmos. & Planetary Sciences
20 Oxford Street
Cambridge, MA 02138

Prof. John Ebel
Department of Geology & Geophysics
Boston College
Chestnut Hill, MA 02167

Eric Fielding
SNEE Hall
INSTOC
Cornell University
Ithaca, NY 14853

Dr. Mark D. Fisk
Mission Research Corporation
735 State Street
P.O. Drawer 719
Santa Barbara, CA 93102

Prof Stanley Flatte
Applied Sciences Building
University of California, Santa Cruz
Santa Cruz, CA 95064

Dr. John Foley
NER-Geo Sciences
1100 Crown Colony Drive
Quincy, MA 02169

Prof. Donald Forsyth
Department of Geological Sciences
Brown University
Providence, RI 02912

Dr. Art Frankel
U.S. Geological Survey
922 National Center
Reston, VA 22092

Dr. Cliff Frolich
Institute of Geophysics
8701 North Mopac
Austin, TX 78759

Dr. Holly Given
IGPP, A-025
Scripps Institute of Oceanography
University of California, San Diego
La Jolla, CA 92093

Dr. Jeffrey W. Given
SAIC
10260 Campus Point Drive
San Diego, CA 92121

Dr. Dale Glover
Defense Intelligence Agency
ATTN: ODT-1B
Washington, DC 20301

Dr. Indra Gupta
Teledyne Geotech
314 Montgomery Street
Alexanderia, VA 22314

Dan N. Hagedon
Pacific Northwest Laboratories
Battelle Boulevard
Richland, WA 99352

Dr. James Hannon
Lawrence Livermore National Laboratory
P.O. Box 808
L-205
Livermore, CA 94550

Dr. Roger Hansen
HQ AFTAC/TTR
Patrick AFB, FL 32925-6001

Prof. David G. Harkrider
Seismological Laboratory
Division of Geological & Planetary Sciences
California Institute of Technology
Pasadena, CA 91125

Prof. Danny Harvey
CIRES
University of Colorado
Boulder, CO 80309

Prof. Donald V. Helmberger
Seismological Laboratory
Division of Geological & Planetary Sciences
California Institute of Technology
Pasadena, CA 91125

Prof. Eugene Herrin
Institute for the Study of Earth and Man
Geophysical Laboratory
Southern Methodist University
Dallas, TX 75275

Prof. Robert B. Herrmann
Department of Earth & Atmospheric Sciences
St. Louis University
St. Louis, MO 63156

Prof. Lane R. Johnson
Seismographic Station
University of California
Berkeley, CA 94720

Prof. Thomas H. Jordan
Department of Earth, Atmospheric &
Planetary Sciences
Massachusetts Institute of Technology
Cambridge, MA 02139

Prof. Alan Kafka
Department of Geology & Geophysics
Boston College
Chestnut Hill, MA 02167

Robert C. Kemerait
ENSCO, Inc.
445 Pineda Court
Melbourne, FL 32940

Dr. Max Koontz
U.S. Dept. of Energy/DP 5
Forrestal Building
1000 Independence Avenue
Washington, DC 20585

Dr. Richard LaCoss
MIT Lincoln Laboratory, M-200B
P.O. Box 73
Lexington, MA 02173-0073

Dr. Fred K. Lamb
University of Illinois at Urbana-Champaign
Department of Physics
1110 West Green Street
Urbana, IL 61801

Prof. Charles A. Langston
Geosciences Department
403 Deike Building
The Pennsylvania State University
University Park, PA 16802

Jim Lawson, Chief Geophysicist
Oklahoma Geological Survey
Oklahoma Geophysical Observatory
P.O. Box 8
Leonard, OK 74043-0008

Prof. Thorne Lay
Institute of Tectonics
Earth Science Board
University of California, Santa Cruz
Santa Cruz, CA 95064

Dr. William Leith
U.S. Geological Survey
Mail Stop 928
Reston, VA 22092

Mr. James F. Lewkowicz
Phillips Laboratory/GPEH
Hanscom AFB, MA 01731-5000(2 copies)

Mr. Alfred Lieberman
ACDA/VI-OA State Department Building
Room 5726
320-21st Street, NW
Washington, DC 20451

Prof. L. Timothy Long
School of Geophysical Sciences
Georgia Institute of Technology
Atlanta, GA 30332

Dr. Randolph Martin, III
New England Research, Inc.
76 Olcott Drive
White River Junction, VT 05001

Dr. Robert Masse
Denver Federal Building
Box 25046, Mail Stop 967
Denver, CO 80225

Dr. Gary McCartor
Department of Physics
Southern Methodist University
Dallas, TX 75275

Prof. Thomas V. McEvilly
Seismographic Station
University of California
Berkeley, CA 94720

Dr. Art McGarr
U.S. Geological Survey
Mail Stop 977
U.S. Geological Survey
Menlo Park, CA 94025

Dr. Keith L. McLaughlin
S-CUBED
A Division of Maxwell Laboratory
P.O. Box 1620
La Jolla, CA 92038-1620

Stephen Miller & Dr. Alexander Florence
SRI International
333 Ravenswood Avenue
Box AF 116
Menlo Park, CA 94025-3493

Prof. Bernard Minster
IGPP, A-025
Scripps Institute of Oceanography
University of California, San Diego
La Jolla, CA 92093

Prof. Brian J. Mitchell
Department of Earth & Atmospheric Sciences
St. Louis University
St. Louis, MO 63156

Mr. Jack Murphy
S-CUBED
A Division of Maxwell Laboratory
11800 Sunrise Valley Drive, Suite 1212
Reston, VA 22091 (2 Copies)

Dr. Keith K. Nakanishi
Lawrence Livermore National Laboratory
L-025
P.O. Box 808
Livermore, CA 94550

Dr. Carl Newton
Los Alamos National Laboratory
P.O. Box 1663
Mail Stop C335, Group ESS-3
Los Alamos, NM 87545

Dr. Bao Nguyen
HQ AFTAC/TTR
Patrick AFB, FL 32925-6001

Prof. John A. Orcutt
IGPP, A-025
Scripps Institute of Oceanography
University of California, San Diego
La Jolla, CA 92093

Prof. Jeffrey Park
Kline Geology Laboratory
P.O. Box 6666
New Haven, CT 06511-8130

Dr. Howard Patton
Lawrence Livermore National Laboratory
L-025
P.O. Box 808
Livermore, CA 94550

Dr. Frank Pilotte
HQ AFTAC/TT
Patrick AFB, FL 32925-6001

Dr. Jay J. Pulli
Radix Systems, Inc.
2 Taft Court, Suite 203
Rockville, MD 20850

Dr. Robert Reinke
ATTN: FCTVTD
Field Command
Defense Nuclear Agency
Kirtland AFB, NM 87115

Prof. Paul G. Richards
Lamont-Doherty Geological Observatory
of Columbia University
Palisades, NY 10964

Mr. Wilmer Rivers
Teledyne Geotech
314 Montgomery Street
Alexandria, VA 22314

Dr. George Rothe
HQ AFTAC/TTR
Patrick AFB, FL 32925-6001

Dr. Alan S. Ryall, Jr.
DARPA/NMRO
3701 North Fairfax Drive
Arlington, VA 22209-1714

Dr. Richard Sailor
TASC, Inc.
55 Walkers Brook Drive
Reading, MA 01867

Prof. Charles G. Sammis
Center for Earth Sciences
University of Southern California
University Park
Los Angeles, CA 90089-0741

Prof. Christopher H. Scholz
Lamont-Doherty Geological Observatory
of Columbia University
Palisades, CA 10964

Dr. Susan Schwartz
Institute of Tectonics
1156 High Street
Santa Cruz, CA 95064

Secretary of the Air Force
(SAFRD)
Washington, DC 20330

Office of the Secretary of Defense
DDR&E
Washington, DC 20330

Thomas J. Sereno, Jr.
Science Application Int'l Corp.
10260 Campus Point Drive
San Diego, CA 92121

Dr. Michael Shore
Defense Nuclear Agency/SPSS
6801 Telegraph Road
Alexandria, VA 22310

Dr. Matthew Sibol
Virginia Tech
Seismological Observatory
4044 Derring Hall
Blacksburg, VA 24061-0420

Prof. David G. Simpson
IRIS, Inc.
1616 North Fort Myer Drive
Suite 1440
Arlington, VA 22209

Donald L. Springer
Lawrence Livermore National Laboratory
L-025
P.O. Box 808
Livermore, CA 94550

Dr. Jeffrey Stevens
S-CUBED
A Division of Maxwell Laboratory
P.O. Box 1620
La Jolla, CA 92038-1620

Lt. Col. Jim Stobie
ATTN: AFOSR/NL
Bolling AFB
Washington, DC 20332-6448

Prof. Brian Stump
Institute for the Study of Earth & Man
Geophysical Laboratory
Southern Methodist University
Dallas, TX 75275

Prof. Jeremiah Sullivan
University of Illinois at Urbana-Champaign
Department of Physics
1110 West Green Street
Urbana, IL 61801

Prof. L. Sykes
Lamont-Doherty Geological Observatory
of Columbia University
Palisades, NY 10964

Dr. David Taylor
ENSCO, Inc.
445 Pineda Court
Melbourne, FL 32940

Dr. Steven R. Taylor
Los Alamos National Laboratory
P.O. Box 1663
Mail Stop C335
Los Alamos, NM 87545

Prof. Clifford Thurber
University of Wisconsin-Madison
Department of Geology & Geophysics
1215 West Dayton Street
Madison, WS 53706

Prof. M. Nafi Toksoz
Earth Resources Lab
Massachusetts Institute of Technology
42 Carleton Street
Cambridge, MA 02142

Dr. Larry Turnbull
CIA-OSWR/NED
Washington, DC 20505

Dr. Gregory van der Vink
IRIS, Inc.
1616 North Fort Myer Drive
Suite 1440
Arlington, VA 22209

Dr. Karl Veith
EG&G
5211 Auth Road
Suite 240
Suitland, MD 20746

Prof. Terry C. Wallace
Department of Geosciences
Building #77
University of Arizona
Tuscon, AZ 85721

Dr. Thomas Weaver
Los Alamos National Laboratory
P.O. Box 1663
Mail Stop C335
Los Alamos, NM 87545

Dr. William Wortman
Mission Research Corporation
8560 Cinderbed Road
Suite 700
Newington, VA 22122

Prof. Francis T. Wu
Department of Geological Sciences
State University of New York
at Binghamton
Vestal, NY 13901

AFTAC/CA
(STINFO)
Patrick AFB, FL 32925-6001

DARPA/PM
3701 North Fairfax Drive
Arlington, VA 22203-1714

DARPA/RMO/RETRIEVAL
3701 North Fairfax Drive
Arlington, VA 22203-1714

DARPA/RMO/SECURITY OFFICE
3701 North Fairfax Drive
Arlington, VA 22203-1714

HQ DNA
ATTN: Technical Library
Washington, DC 20305

Defense Intelligence Agency
Directorate for Scientific & Technical Intelligence
ATTN: DTIB
Washington, DC 20340-6158

Defense Technical Information Center
Cameron Station
Alexandria, VA 22314 (2 Copies)

TACTEC
Battelle Memorial Institute
505 King Avenue
Columbus, OH 43201 (Final Report)

Phillips Laboratory
ATTN: XPG
Hanscom AFB, MA 01731-5000

Phillips Laboratory
ATTN: GPE
Hanscom AFB, MA 01731-5000

Phillips Laboratory
ATTN: TSML
Hanscom AFB, MA 01731-5000

Phillips Laboratory
ATTN: SUL
Kirtland, NM 87117 (2 copies)

Dr. Michel Bouchon
I.R.I.G.M.-B.P. 68
38402 St. Martin D'Heres
Cedex, FRANCE

Dr. Michel Campillo
Observatoire de Grenoble
I.R.I.G.M.-B.P. 53
38041 Grenoble, FRANCE

Dr. Kin Yip Chun
Geophysics Division
Physics Department
University of Toronto
Ontario, CANADA

Prof. Hans-Peter Harjes
Institute for Geophysic
Ruhr University/Bochum
P.O. Box 102148
4630 Bochum 1, GERMANY

Prof. Eystein Husebye
NTNF/NORSAR
P.O. Box 51
N-2007 Kjeller, NORWAY

David Jepsen
Acting Head, Nuclear Monitoring Section
Bureau of Mineral Resources
Geology and Geophysics
G.P.O. Box 378, Canberra, AUSTRALIA

Ms. Eva Johannisson
Senior Research Officer
National Defense Research Inst.
P.O. Box 27322
S-102 54 Stockholm, SWEDEN

Dr. Peter Marshall
Procurement Executive
Ministry of Defense
Blacknest, Brimpton
Reading FG7-FRS, UNITED KINGDOM

Dr. Bernard Massinon, Dr. Pierre Mechler
Societe Radiomana
27 rue Claude Bernard
75005 Paris, FRANCE (2 Copies)

Dr. Svein Mykkeltveit
NTNT/NORSAR
P.O. Box 51
N-2007 Kjeller, NORWAY (3 Copies)

Prof. Keith Priestley
University of Cambridge
Bullard Labs, Dept. of Earth Sciences
Madingley Rise, Madingley Road
Cambridge CB3 OEZ, ENGLAND

Dr. Jorg Schlittenhardt
Federal Institute for Geosciences & Nat'l Res.
Postfach 510153
D-3000 Hannover 51, GERMANY

Dr. Johannes Schweitzer
Institute of Geophysics
Ruhr University/Bochum
P.O. Box 1102148
4360 Bochum 1, GERMANY